Neuroscience and Biobehavioral Reviews 47 (2014) 485–505

Contents lists available at ScienceDirect

Neuroscience and Biobehavioral Reviews

journal homepage: www.elsevier.com/locate/neubiorev

Review

Cellular and molecular neuropathology of the cuprizone mouse model: Clinical relevance for multiple sclerosis

Jelle Praet[a,b,c,*], Caroline Guglielmetti[a,b,c], Zwi Berneman[a,b], Annemie Van der Linden[c], Peter Ponsaerts[a,b]

[a] Experimental Cell Transplantation Group, Laboratory of Experimental Hematology, University of Antwerp, Antwerp, Belgium
[b] Vaccine and Infectious Disease Institute (Vaxinfectio), University of Antwerp, Antwerp, Belgium
[c] BioImaging Laboratory, University of Antwerp, Antwerp, Belgium

ARTICLE INFO

Article history:
Received 31 July 2014
Received in revised form
18 September 2014
Accepted 1 October 2014
Available online 14 October 2014

Keywords:
Cuprizone
Oligodendrocyte
Myelin
Metabolic stress
Neuroinflammation
Demyelination
Remyelination
Multiple sclerosis
Epilepsy
Schizophrenia

ABSTRACT

The cuprizone mouse model allows the investigation of the complex molecular mechanisms behind nonautoimmune-mediated demyelination and spontaneous remyelination. While it is generally accepted that oligodendrocytes are specifically vulnerable to cuprizone intoxication due to their high metabolic demands, a comprehensive overview of the etiology of cuprizone-induced pathology is still missing to date. In this review we extensively describe the physico-chemical mode of action of cuprizone and discuss the molecular and enzymatic mechanisms by which cuprizone induces metabolic stress, oligodendrocyte apoptosis, myelin degeneration and eventually axonal and neuronal pathology. In addition, we describe the dual effector function of the immune system which tightly controls demyelination by effective induction of oligodendrocyte apoptosis, but in contrast also paves the way for fast and efficient remyelination by the secretion of neurotrophic factors and the clearance of cellular and myelinic debris. Finally, we discuss the many clinical symptoms that can be observed following cuprizone treatment, and how these strengthened the cuprizone model as a useful tool to study human multiple sclerosis, schizophrenia and epilepsy.

Contents

* Corresponding author at: Bio-Imaging Lab, University of Antwerp, Campus Drie Eiken (CDE-Uc.114), Universiteitsplein 1, 2610 Antwerp (Wilrijk), Belgium. Tel.: +0032 3 2652762.
E-mail address: jelle.praet@uantwerpen.be (J. Praet).

http://dx.doi.org/10.1016/j.neubiorev.2014.10.004

1. Introduction & historical perspectives

Multiple sclerosis (MS) is generally accepted to be an autoimmune demyelinating disease of the central nervous system (CNS). While the first real medical descriptions of MS date back to the early 18th century, only little progress in understanding MS pathology was made during the 18th and 19th century as research was limited to post-mortem examination of brain tissue from MS patients. During the 20th century however, several immune-mediated animal models for MS were developed like the experimental autoimmune encephalomyelitis (EAE) model and the Theiler murine encephalomyelitis virus model. Besides these, toxin-induced demyelinating models like the cuprizone (bis-cyclohexanone-oxalyldihydrazone, CPZ) model, the lysophosphatidyl choline injection model and the ethidium bromide injection model are often used to investigate the molecular factors contributing to de- and remyelination. The first description of CPZ by Gustav Nilsson dates back to 1950 following his observation that CPZ, which is the condensation product of oxalylhydrazide and cyclohexanone, induced a sensitive blue color reaction upon chelation with copper (Cu) salts (Nilsson, 1950). The first biomedical application however, dates back to 1966 when Carlton observed reproducible low serum Cu levels and demyelination in mice following administration of CPZ (Carlton, 1966). During the following 3 decades, CPZ was mainly used to induce demyelination in Swiss mice, but other mice strains (Albino, BALB/c, BSVS, CD1, ICI & SJL) or animal species (Albino and Wistar rats, guinea pigs and Syrian and Chinese hamsters) were also known to display a variable degree of demyelination upon CPZ intoxication (Adamo et al., 2006; Basoglu et al., 2013; Elsworth and Howell, 1973; Franco et al., 2008; Kanno et al., 2012; Ludwin, 1978; Skripuletz et al., 2011a; Wakabayashi et al., 1977).

Hiremath et al. (1998) published a key study in which the variability of CPZ-induced pathology was reduced to a minimum. In this study, it was determined that feeding 8 week old C57BL/6 mice with a 0.2% CPZ-supplemented diet for 6 weeks consistently induced demyelination with minimal clinical toxicity, making this experimental setup quickly the most used variant of the CPZ mouse model. Following these experiments, 2 experimental setups are now often used on the C57BL/6 background: (i) feeding C57BL/6 mice with a 0.2% CPZ-supplemented diet for 4–6 weeks followed by recovery on a normal diet, resulting in the induction of acute demyelinating lesions followed by spontaneous remyelination and (ii), feeding C57BL/6 mice with a 0.2% CPZ supplemented diet continuously for 12 weeks, resulting in the induction of chronically demyelinated lesions with limited remyelination capacity (Matsushima and Morell, 2001). Acute/chronic demyelination and remyelination, as well as micro- and astrogliosis, following CPZ treatment are represented in Fig. 1.

While the CPZ mouse model has been applied on different animal species and mouse strains during the past 4 decades, currently this model is mainly used on mouse C57BL/6 background as reproducible de- and remyelination is accompanied by microgliosis and astrogliosis. In addition, the availability of many transgenic mouse strains on C57BL/6 background (Table 1), combined with the high reproducibility of the CPZ model on this background, makes CPZ intoxication a favorable model to study both acute and chronic demyelination, as well as remyelination.

2. CPZ-induced metabolic stress predisposes oligodendrocytes to apoptosis

While it is generally accepted that CPZ induced toxicity originates from a perturbation of the very active metabolism in OLGs, no real consensus exists yet concerning the actual modus operandi of CPZ. Within the following chapter, we unify all current knowledge concerning the biochemical and molecular events triggered by CPZ administration, and how these eventually lead to OLG apoptosis and demyelination.

2.1. Physico-chemical behavior of CPZ

Cu, as a cofactor for various cuproenzymes, plays a very important role in many cellular processes and therefore has its concentration tightly regulated within the cell. A disturbed Cu homeostasis can result in neurodegeneration, as for example observed in Wilson's and Menkes disease. Therefore, it is tempting to assume that CPZ-induced pathology originates either from Cu buildup due to entrapment within the cell or from Cu deficiency due to chelation (Rossi et al., 2004). To date, two hypotheses regarding the physico-chemical behavior of CPZ have been investigated.

The first hypothesis suggests that CPZ-induced pathology originates from Cu deficiency. The authors of this hypothesis proposed that CPZ induces a functional Cu deficit as: (i) they could not detect CPZ in brain and liver extracts or serum samples from CPZ-treated mice, and (ii) the chelation of Cu^{2+} by CPZ resulted in precipitating CPZ-Cu^{2+} oligomers in the gastrointestinal tract (Benetti et al., 2010; Taylor et al., 2010b; Venturini, 1973). However, the second hypothesis states that Cu is chelated by CPZ as Cu^{3+} and requires 2 CPZ molecules for each Cu atom bound. Zatta et al. (2005) proposed that CPZ had to be present in the brain as: (i) they could detect CPZ in blood plasma, (ii) a 5-fold increase in brain Cu concentrations after 9 months of a very mild CPZ treatment was observed due to CPZ-Cu oligomer precipitation, and (iii) the hydrazone group of CPZ will be partially hydralized upon binding of Cu, giving rise to the corresponding hydrazide, and CPZ has to be present within the brain for hydrazide-dependent enzyme inhibition to occur (Messori et al., 2007).

Summarizing, the pathological effects of CPZ treatment are due to: (i) in situ disturbance of Cu homeostasis, and (ii) a neurotoxic effect due to enzyme inhibition. However, given the existence of two contradictory hypotheses, further research will be required to fully elucidate the physico-chemical behavior CPZ.

2.2. Megamitochondria and oxidative stress

Suzuki (1969) was the first to report that CPZ induces the formation of megamitochondria in liver tissue of mice (Petronilli

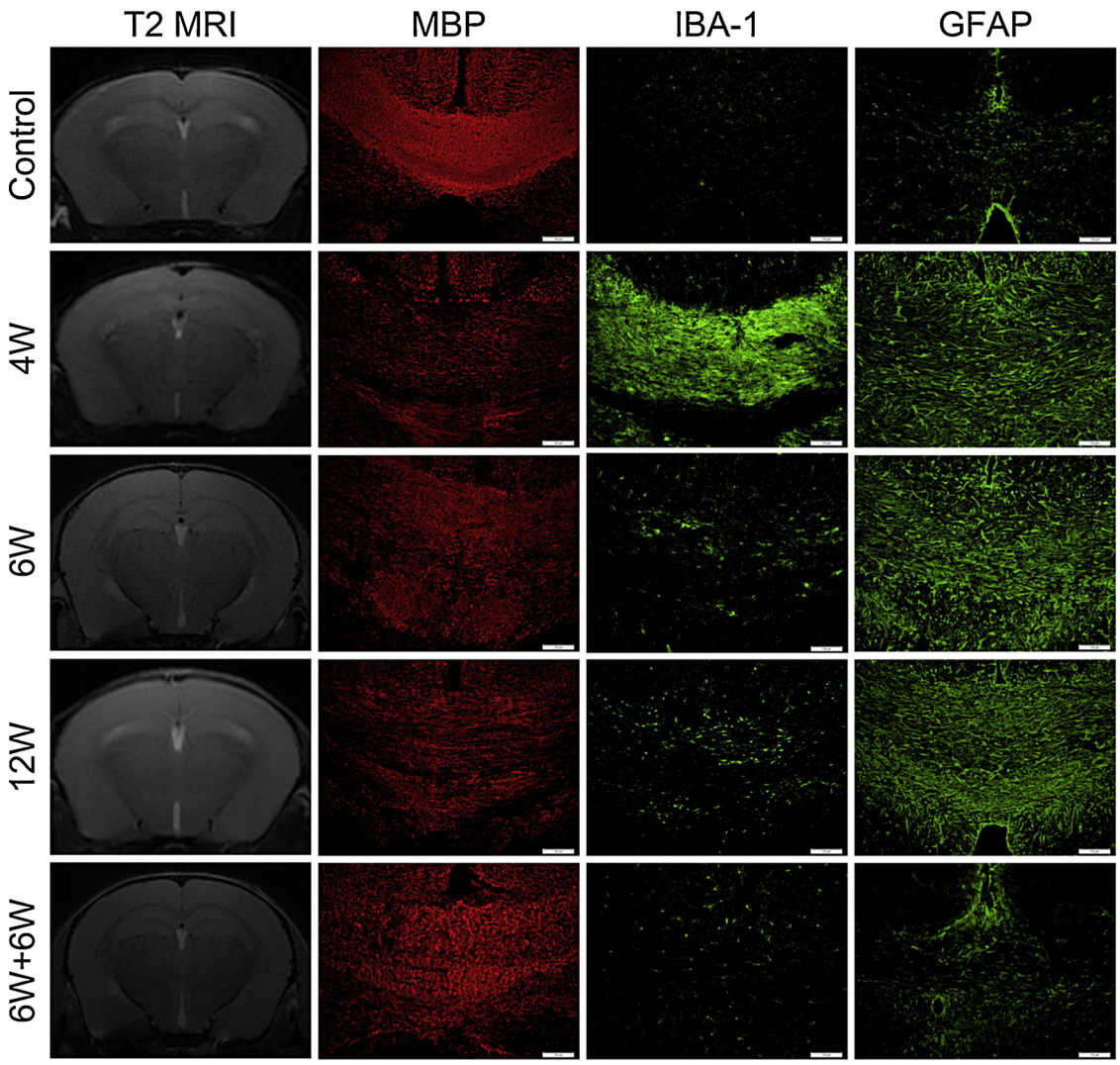

Fig. 1. Representative overview showing myelin content (T2 MRI image and MBP staining), microgliosis (IBA-1 staining) and astrogliosis (GFAP staining) at different time points following feeding of 8-week old female C57BL6/J mice with a 0.2% cuprizone (CPZ) supplemented diet. During acute demyelination (week 4, 4 W), extensive microgliosis and astrogliosis can be observed. By week 6 (6 W) of CPZ treatment, an attempt to remyelinate occurs, while astrogliosis persists in the absence of microgliosis. Administration of CPZ for 12 weeks (12 W) induces extensive demyelination and astrogliosis. However, when mice are allowed to recover for 6 weeks on a normal diet after 6 weeks of CPZ treatment (6 W + 6 W), extensive remyelination occurs, while both microgliosis and astrogliosis disappear. (Scale bars = 100 μm).

and Zoratti, 1990; Tandler and Hoppel, 1975; Wagner and Rafael, 1977). While hepatic megamitochondria in C57BL/6 mice could only be observed following a 0.5% CPZ supplemented diet, the formation of megamitochondria in OLGs was observed already after a 3 week 0.2% CPZ diet (Acs and Komoly, 2012; Biancotti et al., 2008; Hiremath et al., 1998). Megamitochondria formation was however not observed in neurons, astrocytes, cardiac, kidney, kupfer or fat storing cells (Asano et al., 1978; Ludwin, 1978; Tandler and Hoppel, 1973; Wakabayashi et al., 1978). Recent in vitro experiments in which rat primary glial cell cultures were treated with CPZ provided additional proof that microglia, astrocytes and oligodendrocyte precursors cells (OPCs) are unaffected by CPZ while mature OLGs show signs of toxicity upon CPZ treatment (e.g. decreased survival and reduced mitochondrial transmembrane potential) (Benardais et al., 2013; Pasquini et al., 2007).

Inhibition of fission was described as the responsible mechanism for megamitochondria formation (Asano et al., 1978; Flatmark et al., 1980; Miwa et al., 2008; Tandler and Hoppel, 1973; Wakabayashi et al., 1977, 1975). However, mitochondria quickly regained a normal morphology when CPZ treatment was halted (Flatmark et al., 1980; Tandler and Hoppel, 1973; Wakabayashi et al., 1975). In vitro, mitochondria enlarge when subjected to elevated levels of reactive oxygen species (ROS) and reactive nitrogen species (RNS), eventually resulting in the formation of megamitochondria. Therefore, the formation of megamitochondria can be considered as a protective measure of the cell to reduce oxidative stress (Wakabayashi, 2002). Nonetheless, the amount of electrons leaking from the electron transport chain (ETC), and thus $O_2^{\bullet-}$ production, increases dramatically during CPZ treatment due to: (i) an uncoupling of the oxidative phosphorylation process (Tandler and Hoppel, 1973, 1975; Wakabayashi et al., 1975), (ii) a reduced reaction surface (Tandler and Hoppel, 1975), (iii) differences in the cytochrome content (Flatmark et al., 1980; Wagner and Rafael, 1977), and (iv) an inhibition of Complex I–III, Complex II–III and Complex IV (De and Subramanian, 1982; Kimberlin et al., 1976; Millet et al., 2009; Nelecz et al., 1982; Pasquini et al., 2007; Petronilli and Zoratti, 1990; Venturini, 1973; Wakabayashi et al., 1978). In contrast to these observations, Acs et al. (2013) recently described that cuprizone treatment does indeed inhibit Complex IV activity, but not Complex I + III or Complex II + III. Nonetheless, CPZ intoxication clearly imposes an increased oxidative stress on OLGs. In addition, the factors listed below, and shown in Fig. 2, contribute

Table 1
Overview of all transgenic mice strains to which the CPZ model has been applied and how the transgenic background influences demyelination, oligodendrocyte apoptosis, remyelination, microgliosis and astrogliosis.

Phenotype	Demyelination	OLG loss	Remyelination	Microgliosis	Astrogliosis	Reference
Overexpression						
GFAP-C3a	More		Delayed	More	More	Ingersoll et al. (2010)
GFAP-C5a	More		Delayed	More	More	Ingersoll et al. (2010)
GFAP-PDGF-α	Normal		Normal			Woodruff et al. (2004)
	Upon chronic demyelination, remyelination was improved					Vana et al. (2007)
GFAP-sCrry	Less			Less		Briggs et al. (2007)
GFAP/tTA-TRE/IFNγ	Normal	Normal	Less			Lin et al. (2006)
GFAP/tTA-TRE/IFNγ PERK$^{+/-}$	Normal		Less			Lin et al. (2006)
GFAP/tTA-TRE/IFNγ-PLP/Fv2E-PERK	Allows inducible expression of both PERK and IFNγ expression					Lin et al. (2014)
MBP-IFNγ	Less	Less		Less	Less	Gao et al. (2000)
MBP-J37 golli	More	More	More	More	More	Paez et al. (2012)
MT1-IGF1	Normal	Less	Accelerated			Mason et al. (2000b)
GAL-tg	Less	Less				Zhang et al. (2012)
PLP-Fv2E-PERK	Normal	Normal	Normal			Lin et al. (2014)
Knockout						
Phenotype	Demyelination	OLG loss	Remyelination	Microgliosis	Astrogliosis	Reerence
Act1$^{-/-}$	Less			Less		Kang et al. (2012)
Axl$^{-/-}$	Less	Less	Delayed			Hoehn et al. (2008)
BDNF$^{+/-}$	More	Normal	Less	Normal	Normal	VonDran et al. (2011)
Casp1$^{-/-}$	Delayed	Delayed		Delayed	Delayed	Jha et al. (2010)
CCL2$^{-/-}$	Normal microgliosis but reduced macrophage infiltration					Remington et al. (2007)
CCR2$^{-/-}$	Normal microgliosis but reduced macrophage infiltration					Remington et al. (2007)
CIITA$^{-/-}$	Normal cellular infiltration, but no discrimination between inflammatory cell types					Arancibia-Carcamo et al. (2004)
COX-2$^{-/-}$	Less				Less	Palumbo et al. (2011a)
CXCR2$^{-/-}$	Normal	Normal	Normal	Normal	Normal	Lindner et al. (2008)
CXCR2$^{-/-}$	Less	Less				Liu et al. (2010a)
CXCR2$^{-/-}$			Accelerated			Liu et al. (2010b)
Eif2b5$^{R132H/R132H}$			Less		More	Geva et al. (2010)
eNOS$^{-/-}$	Normal	Normal	Delayed	Normal	Normal	Linares et al. (2006)
FcRγ Fyn$^{-/-}$	Less	Less				Seiwa et al. (2007)
FGF2$^{-/-}$	Normal	Normal	More			Armstrong et al. (2006, 2002), Murtie et al. (2005)
	Reduced axonal atrophy upon chronic demyelination					Tobin et al. (2011)
GAS6$^{-/-}$	More	More	Delayed	Accelerated		Binder et al. (2008, 2011)
GnT-IX$^{-/-}$			More		Less	Kanekiyo et al. (2013)
Golli$^{-/-}$	Less	Less	Less	Less	Less	Paez et al. (2012)
I-Aβ$^{-/-}$	Less			Less		Hiremath et al. (2008)
I-Aβ^{tr}	Less			Less		Hiremath et al. (2008)
IFN-αR$^{-/-}$	Normal	Normal	Normal	Normal	Normal	Schmidt et al. (2009)
IFN-β$^{-/-}$	Less	More				Trebst et al. (2007)
IFN-γR$^{-/-}$	Less	Normal	Accelerated	Delayed		Mana et al. (2006)
IKK$^{CNS-/-}$	Less			Less	Less	Raasch et al. (2011)
IL-17$^{-/-}$	Less			Less		Kang et al. (2012)
IL-17R$^{-/-}$	Less			Less		Kang et al. (2012)
IL-18$^{-/-}$	Delayed	Delayed	More	Delayed	Delayed	Jha et al. (2010)
IL-1β$^{-/-}$	Normal	Normal	Less	Normal	Normal	Jha et al. (2010), Mason et al. (2001b)
iNOS$^{-/-}$	More	More		Normal		Arnett et al. (2002)
IRF-8$^{-/-}$	Less	Less		Delayed		Horiuchi et al. (2012)
KLF9$^{-/-}$	Less		Delayed			Dugas et al. (2012)
Lgals3$^{-/-}$	Normal		Less	Increased	Increased	Hoyos et al. (2014)
	While more microglia are present, they fail to switch to an M2 phenotype					
LIF$^{-/-}$	More	More	Less			Marriott et al. (2008)
Ltα$^{-/-}$	Delayed	Delayed	Normal	Delayed	Normal	Plant et al. (2005)
LtβR$^{-/-}$	Delayed		Delayed	Delayed		Plant et al. (2007)
MHC-1$^{-/-}$	Normal	Normal	Normal			Arnett et al. (2003)
MHC-2$^{-/-}$	Normal	Normal	Delayed			Arnett et al. (2003)
MIP-1α$^{-/-}$	Delayed			Delayed	Delayed	McMahon et al. (2001)
Nlrp3$^{-/-}$	Delayed	Delayed	Normal	Less	Delayed	Jha et al. (2010)
nNOS$^{-/-}$	Less	Less	Delayed	Less	Less	Linares et al. (2006)
Noxa$^{-/-}$		Normal		Normal		Hagemeier et al. (2013)
Olig1$^{-/-}$	Normal		Delayed			Arnett et al. (2004)
p53$^{-/-}$	Less	Less				Li et al. (2008)
p75$^{NTR-/-}$	Normal	Normal	Normal			Copray et al. (2005)
p8$^{-/-}$	Delayed	Delayed		Delayed		Plant et al. (2006)
PDGF-αR$^{+/-}$	Normal		Less			Murtie et al. (2005)
Puma$^{-/-}$		Less		Less		Hagemeier et al. (2013)
RAG1$^{-/-}$	Normal	Normal	Normal	Normal		Arnett et al. (2001), Hiremath et al. (2008)
Sema6$^{-/-}$	Less					Bernard et al. (2012)
Sema6$^{+/-}$	Less					Bernard et al. (2012)
St8sialV$^{-/-}$	Normal		Accelerated		Normal	Koutsoudaki et al. (2010)
TG2$^{-/-}$		Normal	Delayed	Normal		Van Strien et al. (2011)

Table 1 (*Continued*)

Phenotype	Demyelination	OLG loss	Remyelination	Microgliosis	Astrogliosis	Reference
TNFα$^{-/-}$	Normal	Delayed	Less	Normal		Arnett et al. (2001), Arnett et al. (2003)
TNFαR1$^{-/-}$	Normal		Normal			Arnett et al. (2001)
TNFαR2$^{-/-}$	Normal		Less			Arnett et al. (2001)
TWEAK$^{-/-}$	Delayed	Less	Delayed	Delayed	Normal	Iocca et al. (2008)
αER$^{-/-}$	Normal	Normal	Normal			Taylor et al. (2010a)
βER$^{-/-}$	Normal	Normal	Normal			Taylor et al. (2010a)
Conditional knockout						
PLP-Notch1$^{-/-}$			Normal			Stidworthy et al. (2004)
PLP-β1 integrin ΔC	Normal		Less			Lee et al. (2006)
SOCS3$^{\Delta MBP/\Delta MBP}$	Less	Less				Emery et al. (2006)
GFAP CreAct1$^{fl/fl}$	Less			Less		Kang et al. (2012)
GFAP-Thymidine kinase	Delayed	Normal	Less	Less		Skripuletz et al. (2013)
PLP-CreER^{T}: FGF1$^{fl/fl}$			More			Mierzwa et al. (2013), Zhou et al. (2012)
GFAP-IκBα-dn	Less			Less	Less	Raasch et al. (2011)
IKK2$^{oligo-/-}$	Normal			Normal	Normal	Raasch et al. (2011)
MOGicrefas$^{fl/fl}$		Normal		Normal	Normal	Hesse et al. (2010)
Myelin visualization						
PLP-eGFP						Crawford et al. (2009), Hussain et al. (2013), Patel et al. (2013)
CNP-eGFP	More			More	More	Millet et al. (2012), Silvestroff et al. (2010)

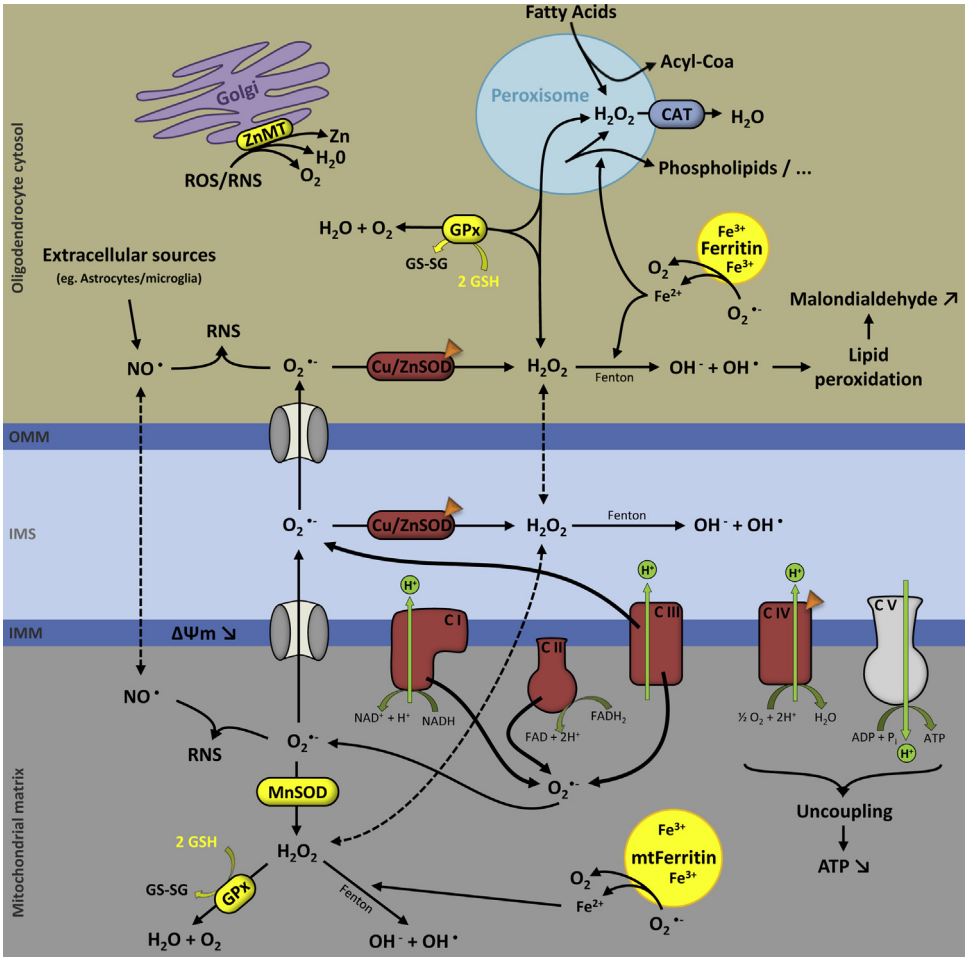

Fig. 2. Schematic overview of molecular changes occurring in oligodendrocyte mitochondria following CPZ treatment (affected enzymes are colored in red). These changes, combined with multiple predisposing factors (colored in yellow), result in an elevated production of ROS/RNS. Dotted lines indicate free diffusion across membranes. Orange triangles mark cuproenzymes. (For interpretation of the references to color in this figure legend, the reader is referred to the web version of this article.)

to the specific vulnerability of OLGs during this increased oxidative stress.

- The rate of $O_2^{\bullet-}$ scavenging and conversion to H_2O_2 is low in OLGs as Manganese Superoxide Dismutase (MnSOD) is present only at low levels (Bernardo et al., 2003; Witherick et al., 2010) and Copper Zinc Superoxide Dismutase (CuZnSOD), a cuproenzyme, has decreased activity during CPZ treatment (Acs et al., 2013; De and Subramanian, 1982; Ljutakova and Russanov, 1985; Russanov and Ljutakova, 1980; Zhang et al., 2008).
- Glutathione peroxidase (GPx) requires glutathione (GSH) as an electron donor for the conversion of H_2O_2 to $H_2O + O_2$. OLGs intrinsically have low amounts of GSH and low GPx activity (Juurlink et al., 1998; Witherick et al., 2010). Moreover, a reduction in GSH content was observed during CPZ treatment (Biancotti et al., 2008).
- As an essential trophic factor for ATP production and lipid synthesis, OLGs have a high amount of intracellular Fe sequestered as Fe^{3+} inside ferritin. Excess $O_2^{\bullet-}$ can however reduce the sequestered Fe^{3+} to Fe^{2+}, thereby releasing the latter into the mitochondrial matrix or cytosol. Subsequently Fe can then initiate and/or propagate lipid peroxidation through Fenton chemistry (Juurlink et al., 1998; Marrif and Juurlink, 2003; Witherick et al., 2010). In vitro, lipid peroxidation can observed by an increase of malondialdehyde upon treatment of OLG cultures with CPZ (Xu et al., 2013).
- Glycerol phosphate dehydrogenase (GPDH) maintains cellular redox potential and plays a role in glycerol production, both of which were found significantly increased following CPZ treatment as a consequence of the cell's response to the increased oxidative stress (Biancotti et al., 2008).
- Peroxisomes, key players in β-oxidation and lipid synthesis, produce high amounts of H_2O_2 which is normally cleared by GPx and peroxisome-bound catalase (CAT). In vitro, CPZ was shown to decrease CAT activity in OLGs cultures (Xu et al., 2013). Additionally, upon OPC maturation the number of peroxisomes increases significantly to allow the OLGs to synthesize the vast amounts of myelin sheath lipids, thereby increasing the production of H_2O_2 and thus the degree of oxidative stress (Juurlink et al., 1998).
- Metallothioneins (MT) fulfill important anti-oxidant functions (Kang, 2006) and while astrocytes show an increased MT1 and MT2 expression following CPZ treatment, OLGs express only low amounts of MTs, which contributes to their oxidative stress vulnerability (Biancotti et al., 2008; Witherick et al., 2010).

2.3. Perikaryon and myelin sheath degeneration

The above described formation of megamitochondria due to CPZ treatment results in an ATP shortage and increasing ROS/RNS concentrations which eventually disrupts proper functioning of the endoplasmatic reticulum (ER). In this chapter we discuss how the combination of oxidative stress and ER stress results in a disturbed protein and lipid synthesis which leads to oligodendrocyte perikaryon degeneration and myelin sheath disintegration.

ER stress during CPZ treatment is characterized by extensive proliferation of the ER and a reduction in hydrophobic protein synthesis (Hemm et al., 1971; Love, 1988; Wagner and Rafael, 1977). ER stress also reduces mRNA transcription/translation to prevent accumulation of un- or misfolded proteins. As such, the downregulation of myelin protein-related mRNAs can be observed already within the first week of CPZ treatment and continues until CPZ treatment is halted (Arnett et al., 2003; Gao et al., 2000; Gudi et al., 2011; Hesse et al., 2010; Jurevics et al., 2001, 2002; Kipp et al., 2009; Morell et al., 1998; Norkute et al., 2009; Seiwa et al., 2007; Selvaraju et al., 2004; Skripuletz et al., 2011b; Tansey et al., 1996). However, misfolded proteins slowly accumulate and eventually trigger the unfolded protein response (UPR), resulting in a massive release of calcium into the cytosol and subsequently OLG cell death (Malhotra and Kaufman, 2007; Matsushima and Morell, 2001; Xu et al., 2005). Of note, while a re-expression of myelin protein mRNAs can be observed during OPC infiltration in demyelinated areas, this only results in myelin protein synthesis if CPZ is withdrawn from the diet (Blakemore, 1984; Ludwin and Sternberger, 1984; Tansey et al., 1997).

Protein synthesis (and thus correct ER functioning) depends on the availability of adequate amino acid levels via the plasma, which in turn depends on correct hepatocyte functioning. As CPZ disturbs normal hepatic functioning (as observed by hepatic megamitochondria), it is no surprise that plasma amino acid levels were altered during CPZ intoxication. As such, a reduction in the plasma levels of alanine, proline and glycine was observed and this triggered the amino acid response pathway (AAR). Activation of the AAR results in phosphorylation of eukaryotic initiation factor 2 (eIF-2α) which can drive both pro- and anti-apoptotic gene expression but foremost, results in a strong reduction of mRNA translation and thus protein synthesis (Goldberg et al., 2013).

Besides the inhibition of myelin protein synthesis, myelin lipid metabolism is affected as well. The major part of the myelin sheath (70%) consists out of lipids with more than a third of these lipids being phospholipids (mainly plasmalogens) that provide structural support and anti-oxidant functions (Baumann and Pham-Dinh, 2001; Farooqui and Horrocks, 2001). Membrane-bound plasmalogens can be hydrolyzed by plasmalogenase leading to an increase of free plasmalogens. Phospholipase A2 (PLA2) can degrade both membrane-bound and free plasmalogens into arachidonic acid (AA), a key intermediate of pro-inflammatory signaling. The activity of both plasmalogenase and PLA2 is increased during CPZ intoxication, thereby contributing to myelin sheath degradation and elevated concentrations of AA (Carey and Freeman, 1983). More specifically, mRNA expression of both secretory PLA2 (sPLA2) and cytosolic PLA2 (cPLA2), but not calcium-dependent PLA2 (iPLA2), is increased. However, an increase at the protein level was observed only for sPLA. Notably, the increase in sPLA occurs at the same time of microglia and astrocyte influx, indicating their contribution to the production of sPLA and the creation of a pro-inflammatory environment. Produced AA will then be further metabolized by cyclooxygenase-1 or -2 (COX-1 and COX-2) into prostaglandin H_2 (PGH2). Although both COX-1 and COX-2 mRNA is upregulated during CPZ-induced demyelination, only COX-1 expression increased at the protein level. However, the exact contribution of COX-1 and COX-2 to the CPZ-induced demyelination process is still not fully unraveled. While COX-1 seemed to be dispensable, COX-2 is required for effective induction of demyelination, as observed in COX-$1^{-/-}$ or COX-$2^{-/-}$ mice. PGH2 can give rise to prostaglandin D2 (PGD2), prostaglandin E2 (PGE2), prostacyclin (PGI2) and thromboxane (TXB2), which are all detectably increased during the demyelination process. Moreover, TXB2 production lasted through subsequent remyelination processes. PGE2 was determined to be the most robustly increased eicosanoid during demyelination, and its signaling via the PGE2-EP2 receptor was demonstrated to contribute to OLG apoptosis. The PGE2-EP2 receptor is expressed by OLGs, astrocytes and microglia and was found upregulated during demyelination, indicating that PGE2 could either contribute directly to OLG apoptosis by EP2 signaling on OLGs or indirectly through stimulation of pro-inflammatory cytokine production by microglia (Palumbo et al., 2011a,b). Alternatively, 5-lipoxenase (5-LO) can convert AA into 5-hydroperoxyeicosatetraenoic acid (5-HPETE), which in turn can give rise to the leukotrienes (LT) LTA_4, LTB_4 and LTC_4. Although 5-LO expression is increased during the demyelination process, inhibition of 5-LO does not prevent demyelination despite reduced interleukin (IL)-6 (but not tumor necrosis factor (TNF)-α or IL-1β) production by microglia.

Nevertheless, these data indicated a role for 5-LO in microglial activation during CPZ induced demyelination (Yoshikawa et al., 2011).

The other two thirds of the myelin lipid pool consists of many different lipids, but foremost of cerebrosides (glycosphingolipids) and cholesterol, for which the concentration also drastically decreases during CPZ treatment. This decrease is in part due to phagocytosis by microglia/macrophages, but also due to the normal turnover of myelin sheath lipids (which are not replenished during CPZ treatment). Very much the same as for the myelin protein gene mRNA levels, ER stress causes a drastic decrease in the mRNA levels of the rate limiting enzymes ceramide galactosyltransferase (CGT) for galactocerebroside synthesis and HMG-CoA reductase for cholesterol synthesis. The mRNA expression of both CGT and HMG-CoA reductase increases again during remyelination, coinciding with the appearance of endogeneous OPCs in areas of demyelination (Carey and Freeman, 1983; Jurevics et al., 2001, 2002; Morell et al., 1998).

As lipid and protein synthesis are inhibited, honeycomb vesiculation of myelin is observed followed by the appearance of intramyelinic vacuoles due to fluid accumulation in between myelin lamellae, thereby splitting these at the intraperiod lines. Fluid also regularly accumulates in the periaxonal space resulting in displacement of the axoplasm, which can cause axonal degeneration (Blakemore, 1972, 1973, 1984; Hemm et al., 1971; Kimberlin et al., 1976; Love, 1988; Ludwin, 1978; Ludwin and Sternberger, 1984; Pattison and Jebbett, 1971; Venturini, 1973). Additionally, autophagocytic and intracytoplasmic vacuoles originating from disrupted myelin lamellae can be observed (Hemm et al., 1971; Ludwin and Sternberger, 1984), along with myelin inner and outer tongue abnormalities like: (i) a large number of stress fibers, (ii) membrane bound bodies, (iii) disorientation of microtubuli, and (iv) vacuoles. Although vacuolation alone was demonstrated to be reversible, demyelination became irreversible following extensive perikaryon degeneration and ultimately leads to OLG apoptosis (Blakemore, 1984). It is important to note that inner and outer tongue abnormalities, OLG perikaryon degeneration, as well as final OLG apoptosis, precede extensive demyelination during CPZ intoxication. This sequence of events is indicative of a primary degeneration of OLGs, rather than a direct autoimmune-mediated attack against myelin proteins. An overview of these degenerative processes is provided in Fig. 3.

2.4. Oligodendrocyte apoptosis

The combined oxidative stress and ER stress results in a degenerating OLG perikaryon and myelin sheath causing notable OLG apoptosis as early as a few days following initiation of CPZ treatment. In contrast, the massive apoptosis of OLGs by week 4 depends on the immune system providing a secondary hit to the already stressed OLGs (see below). Interestingly, by week 6 of CPZ administration OLGs reappear as OPCs differentiate into OLGs (Dupree et al., 2004; Goldberg et al., 2013; Gudi et al., 2011; Hesse et al., 2010; Mason et al., 2000b; Morell et al., 1998). On a sidenote, a 3 week CPZ treatment is sufficient to induce demyelination equal to a 5 week treatment. Therefore, once mature OLGs become perturbed, a sequence of cellular and inflammatory events is triggered leading to OLG apoptosis and demyelination (Doan et al., 2013).

While initially caspase-3 positive fragmented nuclei can be observed, during later stages of CPZ intoxication (post week 3) apoptotic OLGs do not have fragmented nuclei and are caspase-3 negative. This suggests a change from caspase-3 dependent apoptosis to a caspase-3 independent apoptotic process at the time of microglial accumulation (Arnett et al., 2002; Hesse et al., 2010). In addition, while elevated expression of p53, p21 and gadd45 is observed during the first 3 weeks of CPZ intoxication, which is associated with caspase-3 mediated apoptosis, a reduction in OLG apoptosis is noted in $p53^{-/-}$ mice or upon p53 inhibition (Li et al., 2008). p53 mediated apoptosis during CPZ intoxication was shown to be dependent on Puma while Noxa was shown to be dispensable (Hagemeier et al., 2013). Starting from on week 3 post CPZ administration, an increase in poly ADP-ribose polymerase (PARP) activation is observed, while caspase-3 expression (which effectively inhibits PARP) is decreased. The upregulation of PARP will eventually result in apoptosis inducing factor (AIF) mediated apoptosis. In this context, inhibition of PARP was shown to ameliorate OLG loss, indicating a clear role for non caspase-3 dependent apoptosis during the later stage of CPZ intoxication (Veto et al., 2010).

On the other hand, several signaling pathways have displayed protective effects following CPZ intoxication. Leukemia inhibitory factor (LIF) receptor (LIFR) signaling by LIF and ciliary neurotrophic factor receptor (CNTF) has been shown to promote OLG survival but this is usually rapidly terminated by a negative feedback loop mediated by suppressor of cytokine signaling 3 (SOCS3) signaling. As $LIF^{-/-}$ mice showed drastically accelerated OLG loss and $SOCS3^{-/-}$ mice showed increased OLG survival after 3 weeks of CPZ intoxication, it can be concluded that LIF and CNTF fulfill important anti-apoptotic effect following CPZ intoxication (Emery et al., 2006; Gudi et al., 2011; Marriott et al., 2008). Another potent survival signal for mature OLGs is Insulin-like growth factor 1 (IGF-1) which peaks during week 3 to 4.5 following CPZ intoxication. Transgenic mice overexpressing IGF-1 where shown to be protected from OLG apoptosis during CPZ treatment (Gudi et al., 2011; Komoly et al., 1992; Mason et al., 2000a,b). Recently it has also been shown that mice overexpressing Galanin (GAL), a bioactive neuropeptide, suffer only very minor demyelination and OLG loss (Zhang et al., 2012).

Summarizing this chapter, current literature attributes CPZ intoxication to in situ Cu chelation leading to alterations in proper functioning of many different enzymes. This culminates into an increased oxidative stress to which oligodendrocytes in particular are highly sensitive. Next to oxidative stress, CPZ also induces ER stress and together with reduced amino acid levels, this leads to disturbed myelin lipid and protein synthesis and eventually into myelin sheath disintegration. During prolonged increased oxidative stress and ER stress, this process (in combination with a second hit from the immune system, see below) results in OLG apoptosis, despite the presence of pro-survival factors.

3. Neuronal pathology

While neuronal pathology following CPZ-induced demyelination is generally considered to be rare, a body of past and recent literature indicates the contrary. Early on, changes are noticeable at the level of the synapse where neurotransmitter concentrations are disturbed due to alterations in the activity of their synthesizing enzymes (see Fig. 4). Moreover, in demyelinated regions, axonal beading can be observed due to inhibited protein transport, which will eventually lead to axon dystrophy (see Fig. 3). In the following section, several aspects leading to neuronal dysfunction and/or pathology are discussed.

3.1. Neuronal pathology and metabolic coupling between neurons and astrocytes

Young C57BL/6 mice show minimal axonal loss and no reduction in neuronal cell number. In aged C57BL/6 mice however, axonal loss can reach up to 50% and extensive neuron perikaryon degeneration was observed in the hippocampus (Hoffmann et al., 2008; Irvine and Blakemore, 2006). It is however surprising that most neurons survive acute CPZ intoxication while they are equally or even more vulnerable to metabolic perturbation as compared to OLGs. A possible explanation is the metabolic coupling to

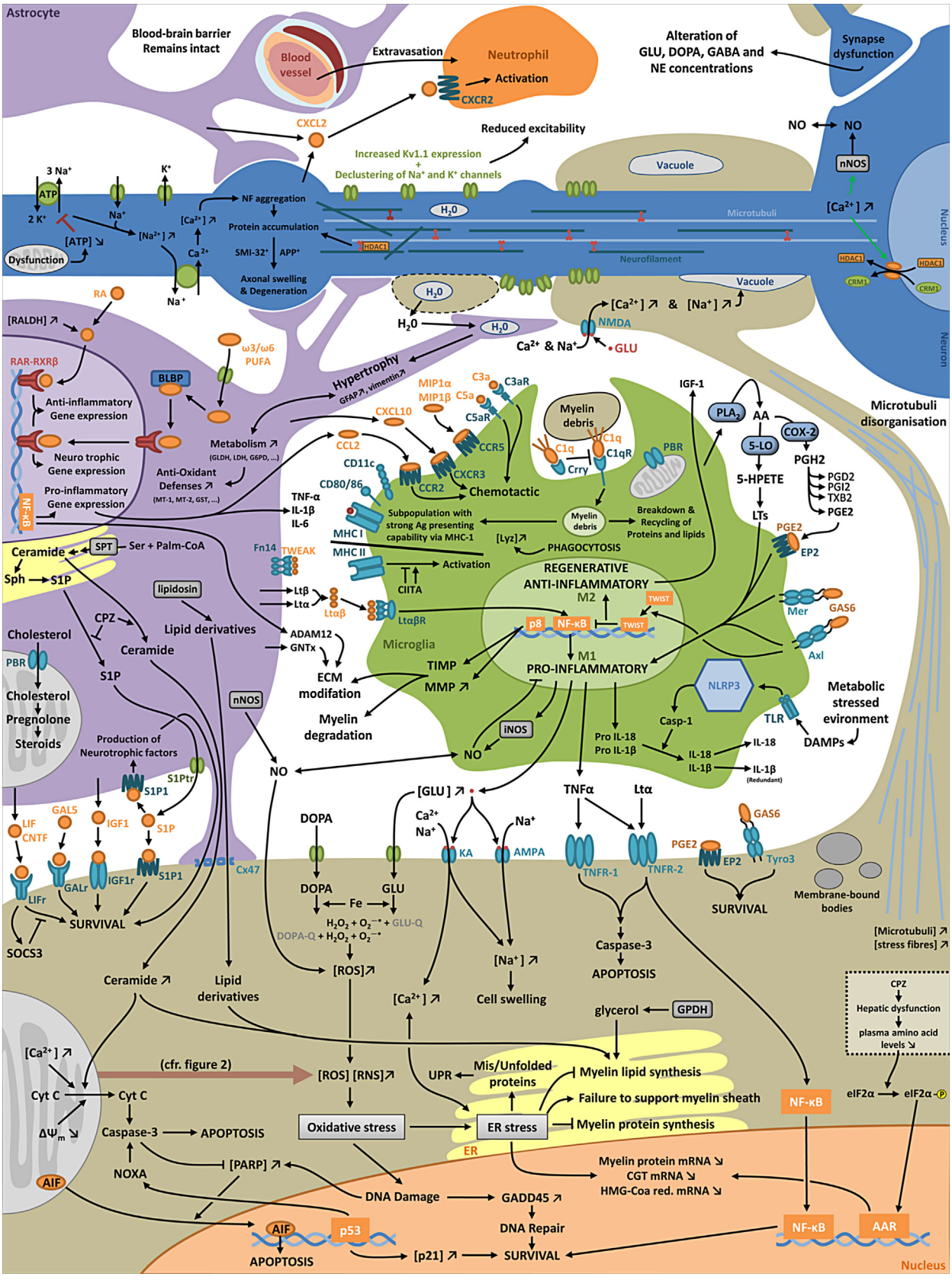

Fig. 3. General schematic overview of the inflammatory cascade following CPZ intoxication and how this sequence of events contributes to demyelination, axonal pathology and oligodendrocyte apoptosis.

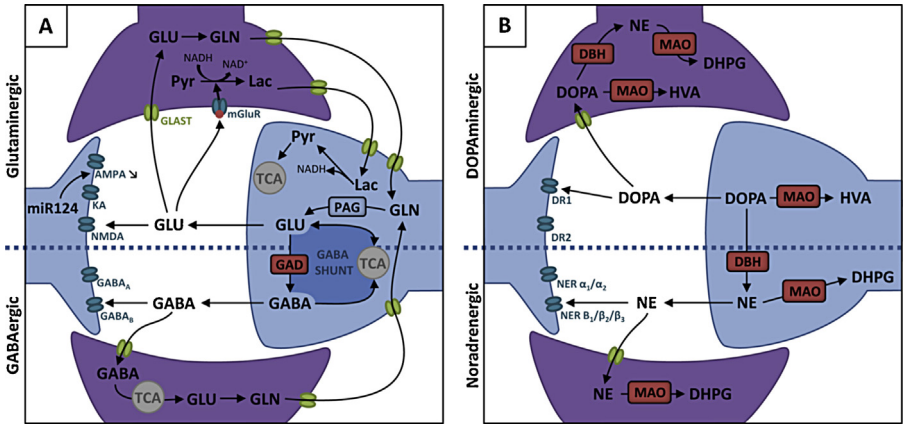

Fig. 4. Schematic overview of CPZ-induced alterations in neuronal synapses. (A) Metabolic coupling of astrocytes and neurons via lactate shuttling provides TCA substrates to neurons and effectively forms a redox buffer, which protects neurons from increased oxidative stress. Inhibition of GAD functioning by CPZ leads to disturbed GLU and GABA concentrations. (B) Inhibition of MAO and DHB by CPZ results in altered DOPA and NE concentrations. Enzymes affected by CPZ are colored in red. (For interpretation of the references to color in this figure legend, the reader is referred to the web version of this article.)

astrocytes, protecting neurons from oxidative stress. It is well described that during metabolic stress, astrocytes can initiate glycolysis by which the formation of a redox buffer protects neurons from oxidative stress (Dewar et al., 2003; Mahad et al., 2008; Marrif and Juurlink, 2003).

3.2. Disturbance of neurotransmitter homeostasis

A glutamine (GLN)–glutamate (GLU)–gamma aminobyturic acid (GABA) cycle (Fig. 4A) exists between neurons and astrocytes because neurons cannot de novo synthesize GLU or GABA (Bak et al., 2006). Just like other hydrazines, CPZ has an inhibitory effect on Glutamic acid decarboxylase (GAD), leading to energy shortage and increased GLU concentration, while suggesting a decreased GABA concentration (Kesterson and Carlton, 1972). This increase in GLU concentration could be responsible for the observed increase in astrocytic glutamate–aspartate transporter (GLAST) expression during demyelination, as astrocytes attempt to keep GLU concentrations at a non-toxic level (Azami Tameh et al., 2013). Neuronal expression of α-amino-3-hydroxy-5-methyl-4-isoxazole propionic acid (AMPA), a GLU receptor, was observed to decrease during demyelination and increase again during remyelination. This process was found to be dependent on microRNA miR-124 and might possibly reflect a neuronal attempt to limit neurotransmitter toxicity during demyelination (Dutta et al., 2013). However, in contrast to the previously described decreased GABA concentration after 8 weeks of CPZ, a recent study observed an increased GABA concentration after 3 weeks of CPZ administration. Although not fully unraveled, this possibly indicates a change in time in neurotransmitter concentrations during CPZ intoxication (Biancotti et al., 2008).

Dopaminergic and noradrenergic synapses (Fig. 4B) are also affected. Dopamine β-hydroxylase (DBH), a cupric enzyme that catalyzes the formation of norepinephrine (NE) from dopamine (DOPA), has a reduced activity during CPZ intoxication. This results in increased DOPA and decreased NE concentrations, as measured in the prefrontal cortex (PFC) as early as 2 weeks following CPZ intoxication (Herring and Konradi, 2011; Xu et al., 2010). Additionally, monoamine oxidase (MAO), important for clearing excessive DOPA and NE, is also inhibited following CPZ intoxication (De and Subramanian, 1982; Herring and Konradi, 2011; Venturini, 1973; Wakabayashi et al., 1978).

Extraccellular GLU and DOPA can be taken up by OLGs and autooxidize by reacting with oxygen, giving rise to their respective quinones which further reduces anti-oxidant defenses. The high Fe concentration in OLGs stimulates this auto-oxidation of neurotransmitters which results in the production of $O_2^{\bullet-}$ and H_2O_2 (Hemdan and Almazan, 2006; Hermida-Ameijeiras et al., 2004; Hider et al., 2008; Spencer et al., 1998; Stankiewicz and Brass, 2009; Troadec et al., 2001). Besides uptake of excess neurotransmitters, OLGs also express GLU receptors like AMPA and kainic acid (KA) receptors, which can lead to cell swelling and excitotoxic cell death. Additionally, functional NMDA receptors were also found on myelin sheaths, thereby allowing Na^+ and Ca^{2+} influx followed by myelin sheath swelling and vacuolation (Dewar et al., 2003).

3.3. Axonal beading

While short term CPZ intoxication induces synaptic dysfunction and disturbed neurotransmitter concentrations, long term CPZ intoxication additionally results in axonal degeneration. Following firing of the neuron, the ATP dependent Na^+K^+ATPase repolarizes the nodes of Ranvier. However, as CPZ intoxication disrupts mitochondrial oxidative energy production, which results in a low ATP supply, Na^+K^+ATPase functioning might become inhibited (Campbell and Mahad, 2011; Irvine and Blakemore, 2006). Combined with a declustering of Na^+ and K^+ channels following demyelination, which increases the energy required to repolarize, this will eventually lead to an elevated intra-axonal Na^+ and Ca^{2+} concentration and thus axonal damage (Crawford et al., 2009; Dupree et al., 2004; Zendedel et al., 2013). In addition, as voltage-activated K^+-channels spread out from their preferred juxtaparanodal position along the demyelinated axon, a disproportionate upregulation is noted in the $K_v1.1$ subunit which results in a temporal dispersion of the compound action potential (CAP). The latter provides a first mechanistic clue behind the reduction in excitability of CPZ-induced demyelinated optic nerves (Bagchi et al., 2014).

A higher intra-axonal Ca^{2+} concentration disrupts axonal transport and causes axonal beading due to: (i) enzymatic dephosphorylation of NFs which causes NF self-aggregation and (ii), CRM1 dependent translocation to the cytoplasm of histone deacetylase (HDAC) HDAC1 (but not HDAC3, HDAC4, HDAC6 or HDAC8), causing inhibition of axonal transport motor proteins (Kim et al., 2010). As such, axonal damage was observed by means of SMI-32 staining while axonal beading was shown via amyloid precursor protein (APP) staining from week 3 of CPZ treatment onwards (Crawford et al., 2009; Kim et al., 2010; Lindner et al., 2008; Merkler et al., 2005; Song et al., 2005; Sun et al., 2006; Tsiperson et al., 2010; Zaaraoui et al., 2008; Zhang et al., 2011). In contrast,

hyperphosphorylation of the microtubuli-associated protein Tau was not observed during CPZ intoxication (Schneider et al., 2004).

Supporting a large axon diameter becomes energetically unfavorable following demyelination and axonal beading resulting. As such, a decrease in axon diameter, associated with decreased expression of NFs, has been observed after 6 weeks CPZ treatment (Cate et al., 2010b; Wu et al., 2008). Both demyelination and a decrease in axon diameter also reduce axonal conduction velocity, as could be observed for callosally projecting neurons of the deeper cortex layers, which only partially recovered during remyelination (Bando et al., 2008).

4. Involvement of the immune system

While it was recently shown that OLG apoptosis occurs already within days following CPZ treatment (thus without extensive microgliosis) (Goldberg et al., 2013), accumulating evidence brought forward that an additional hit from the immune system is required to effectively induce extensive OLG apoptosis by week 4 of CPZ treatment. In vitro, mitochondria and myelin protein synthesis are affected during CPZ intoxication, and although this eventually leads to myelin sheath vacuolation, OLGs do not undergo apoptosis (Cammer, 1999; Pasquini et al., 2007). However, when OLG cell cultures are treated with CPZ in combination with TNFα and/or IFNγ, they show a significant reduction in ETC enzyme activities, an increased ROS production, and – most importantly – effective induction of OLG apoptosis (Pasquini et al., 2007). In vivo, inhibition of microgliosis by minocycline treatment (Skripuletz et al., 2010) and inhibition of neutrophil effector functioning (see below) significantly reduced OLG apoptosis. Both in vitro and in vivo data thus indicate the need for an immune mediated 2nd hit to induce OLG apoptosis. Below, we discuss the role of the immune system during CPZ-induced demyelination and the many effector mechanisms involved (see Fig. 3 and Table 1).

4.1. Neutrophils

CXCR2$^{+/+}$ neutrophils infiltrate the corpus callosum (CC) already during the first week of CPZ intoxication and disappear soon thereafter. Using C57BL/6 CXCR2$^{-/-}$ mice, it was shown that CXCR2$^{+/+}$ neutrophil infiltration was critical to induce OLG apoptosis. Equal metabolic stress and CD45^{+}/Ly6G^{+} neutrophil infiltration were observed between wild type (wt) C57BL/6 and C57BL/6 CXCR2$^{-/-}$ mice, but only wt mice displayed massive OLG apoptosis. Thus, in these studies neutrophil accumulation was shown to be independent of CXCR2, but CXCR2 was critical for neutrophil effector functioning (Liu et al., 2010a; Voss et al., 2012). Although these findings were in contrast with an earlier study describing equal demyelination in CXCR2$^{-/-}$ BALB/c mice, the BALB/c background is known to display only little demyelination upon CPZ intoxication, making it difficult to observe subtle differences (Lindner et al., 2008).

4.2. Astrocytes

Many hypertrophic astrocytes appear at sites where extracellular fluid accumulates from the collapse of intracellular and intramyelinic vacuoles. These astrocytes are characterized by numerous cytoplasmic vacuoles and extensive presence of glial filaments (e.g. GFAP and Vimentin). Their processes are swollen, watery, pale and devoid of organelles, all indicative of fluid uptake in an attempt to restore homeostasis (Blakemore, 1972, 1973; Hemm et al., 1971; Hibbits et al., 2012; Kesterson and Carlton, 1971; Ludwin, 1978). An increase in astrocytic enzyme activity is noted already 1 week after CPZ intoxication, as demonstrated by an increased activity of astrocytic glutamate dehydrogenase (GLDH), NAD(P) diaphorase, lactate dehydrogenase (LDH), glucose-6-phosphate dehydrogenase (G6PD), Complex II of the ETC, metallothionein-1 (MT-1), metallothionein-2 (MT-2) and glutathione-*S*-transferase (GST) (Cammer and Zhang, 1993; Kesterson and Carlton, 1971; Tansey et al., 1997; Zatta et al., 2005). Activation of astrocytes will eventually result in extensive astrogliosis in the CC by week 4 of CPZ intoxication, and astrogliosis persists (although less severe) through remyelination. (Chen et al., 2004; Gudi et al., 2009; Hiremath et al., 1998; Merkler et al., 2005; Zaaraoui et al., 2008).

Astrocytes can become activated following almost any disturbance of brain homeostasis due to the expression of an enormous variety of receptors. These activated astrocytes are able to protect surrounding cells from ATP depletion, oxidative stress and calcium overload. Moreover, astrocytes maintain CNS ionic homeostasis by scavenging excess neurotransmitters and secreting neurotrophic factors which promote cell survival and remyelination (Liberto et al., 2004; Marrif and Juurlink, 2003; Witherick et al., 2010). Concerning the latter, expression of the peripheral benzodiazepine receptor (PBR, also known as TSPO) resulted in mitochondrial cholesterol uptake, the parent compound for steroid synthesis. PBR expression peaked by week 4 of CPZ treatment and gradually disappears thereafter. During remyelination, PBR becomes solely associated with astrocytes while the microglial expression of PBR rapidly decays. As a correlation was found between PBR expression, steroid synthesis and remyelination, astrocytes are thought to provide trophic support during remyelination. (Chen et al., 2004; Chen and Guilarte, 2006; Mattner et al., 2011). This assumption is strengthened by the observation that: (i) intraperitoneal administration of small cholesterol-like compounds, improved remyelination (Li et al., 2013b) and (ii), progesterone administration alleviated demyelination and behavioral deficits (Ye et al., 2013). Another factor corroborating the neuroprotective function of astrocytes is the increase in retinaldehyde dehydrogenase (RALDH) expression during CPZ intoxication. RALDH is implicated in retinoic acid (RA) synthesis, and RA can bind on the RA nuclear receptor, retinoid X receptor β (RXRβ), which controls the expression of many anti-inflammatory genes and was found upregulated specifically in astrocytes (Konig et al., 2012).

Astrocytic lipidosin expression, involved in β-oxidation of fatty acids, and the production of lipid intermediates, is upregulated in actively remyelinating lesions following CPZ intoxication (Song et al., 2007). In addition, many astrocytes positive for brain lipid binding protein (BLBP), involved in ω3 and ω6 PUFA uptake by the cell, are observed in remyelinating lesions. Both these findings stress the role of astrocytes in providing trophic support and substrates for myelin sheath synthesis (Kipp et al., 2011). Ceramide is one of these astrocyte-derived lipid substrates and is de novo synthesized in the ER with serine palmitoyltransferase (SPT) being the rate-limiting enzyme. During CPZ treatment, astrocytes displayed increased SPT expression and accumulated intracellular ceramide. While high concentrations of astrocyte-derived ceramide can sensitize OLGs to apoptotic stimuli, ceramide is also an intermediate for the synthesis of sphingomyelin, cerebrosides and sphingosine (Sph). Sph can be further processed into sphingosine-1-phosphate (S1P) which is implicated in the production of neurotrophic factors as well as OLG proliferation and survival by binding on S1P receptors. While S1P1 receptor expression by OLGs increases during demyelination, the aberrant accumulation of ceramides concomitantly decreases S1P production. In this way, a disturbance in ceramide metabolism might contribute indirectly to OLG apoptosis (Hu et al., 2011; Kim et al., 2011, 2012).

RelA was found activated in astrocytes following demyelination and both IKK2$^{CNS-/-}$ mice and GFAP-IκBα-dn mice, but not IKK2$^{olig-/-}$ mice, showed reduced demyelination following cuprizone intoxication. This suggested that astrocytes contribute

to CPZ toxicity in an NF-κB dependent way. Additionally, it was shown that in IKK2$^{CNS-/-}$ mice the expression of IL-1β, TNFα and CCL2 was reduced, suggesting that NF-κB driven pro-inflammatory gene expression in astrocytes might contribute to OLG apoptosis during CPZ intoxication (Raasch et al., 2011). Two other possible downstream effectors of NF-κB signaling, the pro-inflammatory cytokine IL-6 and neuronal NO synthetase (nNOS), were also found upregulated in astrocytes during CPZ treatment and nNOS, in contrast to endothelial NO synthethase (eNOS), was shown indispensable for CPZ induced OLG apoptosis (Linares et al., 2006; Tezuka et al., 2013). In contrast to the above described deleterious role for NF-κB signaling during CPZ treatment, astrocytes become ADAM12 positive following 5 weeks of CPZ intoxication in an NF-κB-dependent way. This suggests a dual role for NF-κB signaling in astrocytes, as ADAM12 modifies the extra cellular matrix (ECM) to allow OPC infiltration (Baertling et al., 2010). Next to ADAM12, astrocytes were also shown to modify the ECM via O-mannosylation of α-dystroglycans, which was catalyzed by acetylglucosaminyltransferase-IX (GnT-IX). However, in contrast to ADAM12, *O*-mannosyl glucans are inhibitory to remyelination (Kanekiyo et al., 2013).

4.3. Microglia/macrophages

A key study by Hiremath et al. (1998), in which demyelination was induced for the first time in C57BL6/J mice using CPZ, also described extensive microgliosis following CPZ treatment. As such, microgliosis was seen as early as week 2 and peaked by week 4.5, coinciding with massive demyelination and initiation of remyelination. At the peak of microgliosis a large number of proliferating microglia can be observed, although up to 30% of these originate from peripheral progenitors that had adopted a microglial phenotype after lesion infiltration (Hiremath et al., 1998; Matsushima and Morell, 2001; Remington et al., 2007). The infiltration of peripheral macrophages is dependent on the CCR2/CCL2 signaling axis, and CCL2 mRNA expression was upregulated during early CPZ intoxication (Biancotti et al., 2008). However, as microglia and macrophages are phenotypically largely the same, and literature rarely discriminates between the 2 cell populations, we here refer to microglia and/or macrophages as microglia, unless stated otherwise.

Microglia within CPZ-induced lesions have been ascribed both a pro-inflammatory M1 and an anti-inflammatory or regenerative M2 phenotype. The temporal co-existence of both phenotypes of microglia was supported by the detection of differentially expressed receptors and cytokines, like TLR-4, Lyz2, TNF-α, IL-1α, IL-1β and MMP12 indicative for M1 phenotype, and IL-13Rα1, IL-4Rα and IL-2Rγ indicative for M2 phenotype (Arnett et al., 2003; Olah et al., 2012). Importantly, it was shown that myelin debris has a regulatory effect on microglial activation, phagocytosis and thus remyelination (Kotter et al., 2006; Skripuletz et al., 2013), and microglia have been shown to change their phenotype during myelin phagocytosis toward the anti-inflammatory and neurogenesis-stimulating M2 phenotype (Neumann et al., 2009). Additionally, based upon their transcriptome fingerprint microglia exert the following functional tasks: (i) phagocytosis of myelin debris and dead cells, (ii) salvage of myelin constituents, (iii) recruitment of OPCs and trophic support, and (iv) orchestrating tissue remoddeling (Biancotti et al., 2008; Matsushima and Morell, 2001; McMahon et al., 2002; Olah et al., 2012; Voss et al., 2012). As such, microglia are observed at sites of myelin vacuolation where they phagocytize excess fluids and myelin debris. It has to be noted however, that several authors also reported the occurrence of microglial processes in between myelin lamellae, stripping myelin from axons, indicating that microglia might actively take part in myelin breakdown (Blakemore, 1972, 1973; Ludwin, 1978). This process might be driven by the upregulation of the p8 transcription factor, resulting in the expression of matrix metalloproteinases (MMPs) and MMPs are known to stimulate myelin sheath degradation. Additionally, tissue inhibitors of metalloproteinase (TIMPs) are able to inhibit MMPs, and a disturbance of the balance between MMPs and TIMPs has also been noted during CPZ intoxication (Plant et al., 2006; Skuljec et al., 2011).

During CPZ intoxication, microglia in demyelinating lesions display an upregulation of phagocytosis-related proteins and signaling molecules, including lysozyme, triggering receptor expressed on myeloid cells-2 (TREM-2b), CD11b, CD80, toll like receptors (TLRs), FC receptors (FcR), phosphatidylserine receptors (PSRs), scavenger receptors (Srs), complement receptors (Crs) and purine receptors (Prs). As discussed before, the increased phagocytic activity by microglia was subsequently followed by the upregulation of mRNA for myelin-related genes, like MBP and MAG, once more supporting the fact that microglial myelin debris phagocytosis allowed OPCs to initiate differentiation and remyelination (Bedard et al., 2007; Jurevics et al., 2002; Matsushima and Morell, 2001; Morell et al., 1998; Voss et al., 2012). Myelin debris phagocytosis was shown to be, at least partially, dependent on C3a or C5a deposition, indicating a clear role for complement proteins during myelin debris phagocytosis (Ingersoll et al., 2010). During demyelination, deposition of C1q protein was also noted while the expression of soluble Crry protein was abolished, facilitating the complement-mediated myelin debris phagocytosis by microglia (Briggs et al., 2007). Additionally, osteopontin expression peaks by week 3 of CPZ treatment and was also shown to facilitate myelin debris phagocytosis. While the exact mechanism is still unknown, osteopontin was speculated to function as an opsonin (Selvaraju et al., 2004).

As CPZ induces demyelination without T cell involvement, MHC-II expression in this model is directly associated with microglia activation. Defective MHC-II signaling results in reduced microglial TNFα, IL-1β and NO production (Arnett et al., 2003; Bedard et al., 2007; Hiremath et al., 2008; Voss et al., 2012). Additionally, Class II transactivator (CIITA) was shown to effectively control (but not restrict) MHC-II expression during the different stages of CPZ induced demyelination (Arancibia-Carcamo et al., 2004). Of note, although MHC-II was not responsible for antigen presentation, a sub population of microglia was found to express CD11c, a marker for antigen presenting cells in the peripheral immune system. In in vitro experiments, this subpopulation displayed high expression of MHC-I, CD80 and CD86, resulting in strong antigen presenting capabilities (Remington et al., 2007).

The activation of microglia is partially also mediated via astrocytes, providing the necessary signaling environment to trigger microglia recruitment and subsequent myelin debris phagocytosis, a process possibly mediated by CXCL10 signaling (McMahon et al., 2001; Skripuletz et al., 2013). In addition, microglial MIP-1α and MIP-1β expression peaked by week 4 of CPZ treatment as such, microglia themselves amplify microglial accumulation and activation (McMahon et al., 2001). On the other hand, the latter could for example also be responsible for astrocytic IL-6 production as described earlier. Microglia also express a wide range of danger-associated molecular patterns (DAMPs) which allow them to sense the CPZ induced metabolic stress and subsequently become activated. Following CPZ treatment, microglial DAMP activation triggers an increase in NLRP3 inflammasome formation, and subsequently an increase of caspase-1 activation and the production of IL-1β and IL-18. Where NLRP3, caspase-1 and IL-18 were shown necessary for demyelination, IL-1β was shown to be dispensable despite being present at elevated concentrations during CPZ-induced demyelination. In contrast, where IL-18 was shown detrimental for remyelination, IL-1β was shown to be an important factor in promoting remyelination (Jha et al., 2010; Mason et al., 2001b). Lastly, growth arrest-specific protein 6 (GAS6) signals via its receptors Tyro3, Mer and Axl. Microglial Axl (but not Tyro3)

signaling was shown important for microglia accumulation and phagocytosis of myelin debris during CPZ treatment. In contrast, Tyro3 expression by OLGs was shown an important pro-survival signaling pathway, and absence of GAS6 significantly delayed remyelination following CPZ induced demyelination (Binder et al., 2008, 2011; Hoehn et al., 2008; Tsiperson et al., 2010).

As a major microglial effector molecule, TNFα readily induces apoptosis in CPZ treated OLG cultures, consistent with TNFα signaling via TNFR-1 (Pasquini et al., 2007). However, while the apoptosis promoting TNFR-1 is found constitutively on OLGs, an upregulation of TNFR-2 on OLGs was seen during de- and remyelination, thereby promoting OLG survival. These data clearly indicate a dual role for microglial TNFα signaling during de- and remyelination (Arnett et al., 2001; Plant et al., 2005). Additionally, it was recently shown that TNFR-2 activation on astrocytes is required for astrocytic CXCL12 production, which then binds on CXCR4 expressed by OPCs and by doing so induces OPC proliferation and differentiation (Patel et al., 2012). Another member of the TNF superfamily, lymphotoxin-α (LTα), is mainly produced by astrocytes and was shown to be extremely toxic to OLGs in vitro while delaying OLG loss and subsequent microglial accumulation following CPZ treatment (Plant et al., 2005; Voss et al., 2012). Upon interaction of LTα with LTβ within astrocytes, LTαβ is then able to bind the microglial LTβ receptor (LTβR). During CPZ induced demyelination, LTβR expression by microglia was increased and LTβR signaling contributed to demyelination in an NF-κB dependent way (Plant et al., 2007). A third cytokine of the TNF superfamily, TNF-like weak inducer of apoptosis (TWEAK), can exert both pro- and anti-apoptotic functions by binding to its receptor Fn14. Expression of Fn14 was found to be significantly upregulated on astrocytes following CPZ treatment, and TWEAK was suggested to contribute to demyelination by stimulation of microglia accumulation (Iocca et al., 2008).

As a second major effector pathway, microglia produce high amounts of AA metabolites, NO and ROS in response to injury (Liberto et al., 2004). While astrocytic/neuronal nNOS was shown to be crucial for the induction of OLG apoptosis (see above), activated microglia produce substantial higher amounts of NO via inducible NOS (iNOS) and iNOS becomes rapidly upregulated in microglia during CPZ intoxication. Rather unexpectedly however, iNOS was found to protect against demyelination and OLG loss at week 3, but not week 4, of CPZ treatment. This effect might be due to the iNOS-negative feedback system which normally limits pro-inflammatory cytokine expression and compensatory effects of eNOS. These data suggest that effector function(s) of NO might depend on the source and concentration of NO during CPZ intoxication (Arnett et al., 2002; Raposo et al., 2013).

4.4. T and B cells

A leaky blood brain barrier (BBB) is one of the hallmarks of MS pathology as it allows entry of inflammatory cells, among which auto-reactive T cells, into the CNS. However, during CPZ intoxication an intact BBB was shown by HRP leakage, radioactive tracer leakage, serum extravasation and MRI, thereby in part explaining the absence of T and B cell contribution to CPZ induced pathology (Bakker and Ludwin, 1987; McMahon et al., 2002; Merkler et al., 2005; Sansom et al., 1973). Moreover, using RAG$^{-/-}$ mice, deficient in B and T cells, it has been shown multiple times that, in contrast to EAE, B and T cells do not contribute to CPZ induced lesions, as equal demyelination was observed in wt and RAG$^{-/-}$ mice (Arnett et al., 2001; Hiremath et al., 2008; Hiremath et al., 1998; Matsushima and Morell, 2001). During CPZ intoxication, lymphocytes were only a very small fraction (1.5%) of the infiltrating peripheral cell populations (McMahon et al., 2002; Remington et al., 2007). Infiltrating T cells displayed a non-activated phenotype, as determined by the absence of CD44 and CD69 expression (Remington et al., 2007). Additionally, as Cu is required for IL-2 synthesis, it is no surprise that IL-2 mRNA expression is not observed during CPZ intoxication. However, IL-2 has chemoattractant properties and is important for proliferation of activated T cells and as such, the lack of IL-2 can at least partially explain the absence of a contributing T-cell component during CPZ intoxication (Matsushima and Morell, 2001).

However, it is important to note that CPZ-induced demyelination can lead to the generation of myelin reactive T and B cells. For example, myelin specific humoral responses were observed after CPZ-induced demyelination. Moreover, T cells isolated from CPZ treated animals were shown to display decreased IFN-γ and TNF-α expression, but an increased IL-10 expression upon stimulation with myelin antigens. In vivo, resistance to EAE induction was shown upon extensive CPZ induced demyelination. These in vitro and in vivo experiments suggest that CPZ treatment triggers a series of regulatory mechanisms, which drives T cells toward tolerance rather than encephalitogenicity (Mana et al., 2009). Indeed, as described earlier, microglia upregulate their machinery for antigen presentation (MHC-II, CD74, class H2-Aα and class HZ-Aβ1), however the expression levels of co-stimulatory molecules, like CD40 and CD80, remains unchanged on most microglia. Moreover, the inhibitory costimulatory molecule CD247 becomes upregulated (Olah et al., 2012). Recently it was shown that, following NLRP3 inflammasome-mediated IL-1β and IL-18 production by microglia, CD3^{+} T cells produce IL-17 and in this way amplify the inflammatory cascade. As deficient IL-17 signaling resulted in a reduced demyelination following CPZ treatment, this might indicate a possible role for T cells during CPZ intoxication after all (Kang et al., 2012).

Finally, the role of interferon gamma (IFN-γ), a major pro-inflammatory cytokine produced by T cells and natural killer cells, and one of the most potent activating stimuli for macrophages and microglia, is rather unclear at the moment. IFN-γ receptor (IFN-γR)$^{-/-}$ mice and Irf8$^{-/-}$ mice, a downstream effector of IFN-γ receptor signaling, both displayed delayed microglia accumulation and demyelination, in combination with increased OLG survival, indicating an important role for IFN-γ during non T-cell mediated demyelination (Mana et al., 2006). However, transgenic mice expressing IFN-γ under control of the MBP promotor displayed reduced astrogliosis, microgliosis, OLG apoptosis and demyelination during CPZ intoxication (Gao et al., 2000). Therefore, further research will be needed to determine the exact contribution of IFN-γ signaling to neuroprotection and/or neuroregeneration.

Summarizing this chapter, we here described multiple immune effector systems following CPZ induced metabolic changes. Importantly, neutrophils are observed infiltrating the CNS lesion already after 1 week of CPZ treatment, and together with microglia are the main inducers of OLG apoptosis. However, astrocytes and microglia display a rapid reaction to metabolic perturbations and attempt to restore homeostasis by clearance of cellular/myelin debris and excess fluids. In this context, the removal of myelin and cellular debris is an important pre-requisite for remyelination to occur. In addition, the secretion of neurotrophic factors by immune cells is indispensable for remyelination effective remyelination (see below).

5. Remyelination

Remyelination starts at the onset of OPC accumulation and this coincides with the accumulation of microglia and astrocytes following 3 weeks of CPZ treatment. Subsequently, myelin protein mRNA expression is upregulated by week 5, when OPCs start differentiating. Remyelination becomes apparent by week 6 of CPZ treatment as the newly formed OLGs become mature, myelinating OLGs (Mason et al., 2000a; Matsushima and Morell, 2001; Skripuletz

et al., 2011a). This temporal coincidence suggests a link between inflammation and remyelination, which is further supported by the fact that remyelination in wild type mice is much more effective as compared to remyelination in TNFα$^{-/-}$ and MHC-2$^{-/-}$ mice following CPZ-induced demyelination (Arnett et al., 2003). This link can also be speculated from a growth factor expression analysis during CPZ intoxication. NRG1, GDNF and CNTF are upregulated early on and thought to induce astrocytic LIF production, which in turn activates microglia to release IGF-1, FGF2, and HGF (Gudi et al., 2011). Additionally, microglia were shown important for an efficient remyelination process as microglia inhibition via minocycline treatment prohibited microglial CNTF production, and eventually hampered remyelination (Tanaka et al., 2013).

Paradoxically, OPCs survive during CPZ treatment while they are more susceptible to oxidative stress as compared to mature OLGs. Although OPCs express higher levels of $O2^{\bullet-}$ scavenging MnSOD, they display an estimated 8 fold less H_2O_2 scavenging CAT activity as compared to OLGs (Bernardo et al., 2003; Butts et al., 2008). Nonetheless, OPCs themselves survive CPZ treatment as their metabolism is much slower compared to mature OLGs. Upon differentiation however, the newly formed OLGs become subjected to a much higher oxidative stress and ER stress as they attempt to synthesize the vast amounts of proteins and lipids required to produce the myelin sheaths, and this eventually results in the cell death of these newly formed OLGs (Benardais et al., 2013; Butts et al., 2008; Juurlink et al., 1998). As such, during remyelination, ER stress was only observed in newly formed OLGs by the expression of binding immunoglobulin protein (BiP), CAATT enhancer-binding protein homologous protein (CHOP) and eIF-2α. Binding of the ER chaperone BiP to misfolded proteins will release BiP from PERK and eventually results in the phosphorylation of eIF-2α. The latter then causes attenuation of mRNA transcription and the initiation of the UPR as the cell tries to survive. However, when ER stress cannot be resolved due to continuous CPZ treatment, the UPR will result in CHOP expression and thus eventually OLG apoptosis. Of note, PERK overexpression was found to potently protect remyelinating OLGs from the deleterious effects of IFN-γ (Lin et al., 2006, 2014). Lastly, inhibition of the 26S proteasome was seen to result in an arrest of OPC proliferation and stimulated their differentiation (Millet et al., 2009; Pasquini et al., 2003).

The OPCs found in demyelinated lesions can be either endogeneous to the tissue, originate from nearby unaffected tissue or originate from germinal locations like the subventricular zone (SVZ), the subcallosal zone (SCZ) or the hippocampal subgranular zone (SGZ). Proliferating OPCs are observed in demyelinated lesions between week 1 and 5 of CPZ administration, but also in the aforementioned germinal zones from which OPCs are thought to migrate toward the demyelinating lesions (Islam et al., 2009; Kumar et al., 2007; Mason et al., 2000a; Murtie et al., 2005; Silvestroff et al., 2010; Vana et al., 2007; Woodruff et al., 2004). For the SVZ in particular, an increased progenitor cell proliferation in response to CPZ treatment was observed, but these cells accumulated in the olfactory bulb rather than the splenium following CPZ-induced demyelination. Therefore, this study supported the notion that it is most likely tissue endogeneous OPCs which are responsible for the spontaneous remyelination (Guglielmetti et al., 2013). Interestingly, under demyelinating conditions where OLGs survive, no OPC accumulation is observed, indicating that OLG apoptosis, but not demyelination, is a necessary trigger for OPC accumulation to occur (Mason et al., 2000b).

During development, myelination occurs following a strict growth factor expression scheme which finally results in the formation of myelinating OLGs (Trapp et al., 1997). The same is true for remyelination following CPZ treatment although differences can be noted. As such, remyelination is initiated by the proliferation and migration of OPCs toward the lesion site. This process, at least in the CPZ model, was shown to be dependent on signaling by golli myelin basic protein (Paez et al., 2012), T3 hormone dependent gene expression (Franco et al., 2008; Harsan et al., 2008; Silvestroff et al., 2012) and the stimulation by BDNF (Gudi et al., 2011; VonDran et al., 2011). In contrast, CXCR2 signaling by non-hematopoietic cells was shown to be deleterious to OPC lesion repopulation as CXCR2$^{-/-}$ mice displayed improved OPC distribution (Liu et al., 2010b).

Following the accumulation of OPCs at demyelinated lesions, OPCs will start to differentiate toward OLGs and many proteins and transcription factors were seen to play a role in this process. As such, the transcription factor Olig-2 and its downstream effector Zinc finger protein 488 (Zfp488) were observed to be critical to OPC differentiation into OLGs (Chen et al., 2012; Soundarapandian et al., 2011). Kruppel-like factor 9 (Klf9), another zinc finger containing transcription factor, is induced by the earlier mentioned T3 hormone, and was also shown required for efficient differentiation of OPCs into OLGs (Dugas et al., 2012). In addition, ECM modification by tissue transglutaminase (tTG) was shown important for OLG process elongation and branching (Van Strien et al., 2011). In contrast, posttranslational modification of the neural cell adhesion molecule (NCAM) by polysialic acid (PSA, synthesized by St8siaIV) (Koutsoudaki et al., 2010), or the expression of LINGO-1 were seen to inhibit OPC differentiation toward OLGs (Mi et al., 2009). When LINGO-1 dimerizes with p75NTR in the presence of myelin proteins, they are known to inhibit neurite outgrowth (Lu et al., 2005) but the effect of only p75NTR signaling on remyelination remains unknown and requires further investigation (Petratos et al., 2004). Besides the critical importance of the above mentioned factors, the necessity of several immune-cell derived molecules and proteins for OPC differentiation has also been shown. As such, the microglial expression of galectin 3 was shown critical to OPC differentiation. Whether this was due to a direct effect on OLGs or the induction of microglia to adopt an M2 phenotype (or a combination of both) remains to be elucidated (Hoyos et al., 2014; Pasquini et al., 2011). Additionally, the major microglial effector molecule GLU has its NMDA receptor expressed by NG2^{+} OPCs and was shown necessary for OPC differentiation (Li et al., 2013a). Lastly, CXCL12 signaling via CXCR4 on OPCs also induced OPC differentiation. As astrocytes produce CXCL12 in human MS lesions, these authors hypothesized that astrocytes might be responsible for CXCL12 production during CPZ treatment as well, but this remains to be proven (Patel et al., 2010).

The last part of the transcriptional program during remyelination covers the maturation of these newly formed OLGs into fully mature, myelinating OLGs. A large portion of the newly formed OLGs is positive for the transcription factor SOX17, but SOX17 expression is lost once OLGs are fully mature. This suggested that SOX17 is an important initiating factor of OLG maturation (Moll et al., 2013). Another transcription factor, Olig-1, is known to promote OLG process elongation and branching (Othman et al., 2011), and was shown to contribute to OLG maturation during remyelination (Arnett et al., 2004). Lastly, the presence of BDNF (Gudi et al., 2011; VonDran et al., 2011) and IL-11 (Maheshwari et al., 2013) were shown to promote OLG maturation, while galectin 1 inhibited OLG maturation (Pasquini et al., 2011).

While the above described factors thus have a straightforward function during remyelination, some proteins were seen to exert a dual function or even a not yet fully elucidated function. As such, FGF2 signaling via FGF receptor 1 was attributed a dual function as it was shown to stimulate OPC proliferation but to inhibit differentiation into myelinating OLGs (Armstrong et al., 2006, 2002; Gudi et al., 2011; Mierzwa et al., 2013; Tobin et al., 2011; Zhou et al., 2012). In addition to FGF2, PDGF-α signaling was found to stimulate OPC proliferation but also contributed to the maturation of OPCs into myelinating OLGs. Therefore it was proposed that while PDGF-α is critical to OPC proliferation and accumulation,

FGF2 is synergistic the PDGF-α mediated accumulation of OPCs as it prevents further maturation of OPCs into OLGs (Kumar et al., 2007; Murtie et al., 2005; Vana et al., 2007; Woodruff et al., 2004). Bone morphogenic protein 4 (BMP4) exerted a dual function as well, as it stimulated OPC proliferation while inhibiting OPC differentiation. As a sidenote, BMP4 apparently also fulfilled a role during demyelination, as the phosphorylation of its downstream effector proteins SMAD1, SMAD5 and SMAD8 indicated active BMP4 signaling (Cate et al., 2010a; Sabo et al., 2013, 2011). The pro-inflammatory IL-1β on the other hand, was shown redundant for demyelination while it stimulated IGF-1 production and in this way contributed to remyelination (Komoly et al., 1992; Mason et al., 2001b; Matsushima and Morell, 2001). Unexpectedly, Jagged 1 (Stidworthy et al., 2004) and semaphorin 6A (Bernard et al., 2012) did not influence any stage of the remyelination process.

Following the above described initial spontaneous attempt at remyelination, and during continued CPZ treatment, a 2nd wave of OLG apoptosis is noted around week 8 which is again quickly followed by another spontaneous attempt at remyelination starting between week 10 and 12. However, this 2nd attempt is much smaller in comparison with the observed remyelination after acute demyelination. The latter can be explained by: (i) depletion of the OPC population, (ii) the presence and/or absence of respectively inhibitory and/or stimulatory signals for OPC proliferation and differentiation, and (iii) the inability of OPCs to migrate into the lesions due to the absence of inflammatory signals triggering cell migration (Biancotti et al., 2008; Blakemore and Irvine, 2008; Kipp et al., 2011; Ludwin, 1980; Mason et al., 2001a, 2004). Additionally, MS patients shown an age-associated decrease in remyelination efficiency during subsequent demyelinating attacks. This was also observed in the CPZ model as older mice show impaired HDAC1 and HDAC2 recruitment which results in the accumulation of the transcriptional inhibitors Hes1, Hes5, Id2 and Id4 in OPCs following demyelination, and this will eventually prevent myelin gene expression (Shen et al., 2008).

Therefore, timely remyelination has become an important therapeutic goal as it reduces the extent of axonal degeneration (Irvine and Blakemore, 2008). Crawford et al. (2009) suggested that for remyelination to be effective in restoring axonal conduction, a critical timewindow exists. As such, when CPZ was administered for only 1.5 weeks, no disorganization of the node of Ranvier was seen and CAPs of callosally projecting neurons were able to fully recover. However when CPZ was administered for 3 or 6 weeks, node of Ranvier disorganization persisted and CAPs did not fully recover, indicating permanent axonal damage. In contrast to this, it was recently described that both paranodal and juxtaparanodal protein organization are nonetheless able to fully recover during remyelination (Zoupi et al., 2013). The occurrence of long lasting deficits is emphasized by the observation that mice undergoing demyelination during a 5 week CPZ treatment period, fully recovered on the motor skill sequence test (MOSS) during remyelination. However, 28 weeks after the cessation of CPZ intoxication, MOSS deficits reappeared (Manrique-Hoyos et al., 2012). These apparently contradictory results stress the need for further research on the long lasting effects of a demyelinating event, even when full remyelination has occurred. (Koutsoudaki et al., 2010).

In summary, this chapter describes the key factors modulating the different stages of remyelination (Fig. 5). Additionally, despite remyelination to occur spontaneously, it is less effective in older mice or during subsequent inflammatory demyelinating attacks. However, when remyelination occurs outside the critical time window, long lasting neurological deficits develop.

6. Morphological and clinical manifestations after cuprizone intoxication

CNS demyelination can result in a plethora of clinical symptoms dependent on: (i) the area that becomes demyelinated, (ii) the degree of de- and remyelination, and (iii) the degree and type of inflammation. These major and minor symptoms will be briefly discussed below.

As described earlier, myelin sheath disintegration occurs through the formation of many vacuoles and these give rise to edema and status spongiosus, as characterized by a fragile and less stiff brain (Carlton, 1966; Ludwin, 1978; Schregel et al., 2012). A severe edematous midbrain leads to stenosis, or even total occlusion of the aquaduct of sylvius. This causes dilution of the 3th and lateral ventricles, hydrocephalus and a domed skull from the resulting pressure (Acs et al., 2009; Hagemeyer et al., 2012; Harsan et al., 2008; Hoffmann et al., 2008; Kesterson and Carlton, 1970; Parenti et al., 2010; Stidworthy et al., 2003; Yu et al., 2004). Additionally, in contrast to the liver, the brain's dry weight became irreversibly reduced by a few percentages following CPZ treatment (Venturini, 1973; Wakabayashi et al., 1975). This reduction in brain volume/weight was also characterized by thinning of the CC and CTX after CPZ intoxication (Fairless et al., 2008; Parenti et al., 2010; Song et al., 2005).

The earliest clinical observation made in the CPZ model was that the severity of symptoms and mortality rate was correlated to the CPZ dose and treatment length (Blakemore, 1973; Carey and Freeman, 1983; Carlton, 1966; Hiremath et al., 1998; Kesterson and Carlton, 1970; Ludwin, 1978; Stidworthy et al., 2003). The age of the mice also had an influence as weanling mice suffered a very severe growth reduction and weight loss following CPZ treatment (Carlton, 1966; Ludwin, 1978). Additionally, older animals were less susceptible to demyelination compared to juvenile mice, and thus required higher doses or a prolonged treatment period for equal pathology to occur (Carlton, 1967, 1969; Pattison and Jebbett, 1971; Wang et al., 2013). The observed weight loss can be explained by a systemic toxic effect of cuprizone or by a reduced food intake (Pattison and Jebbett, 1971; Wakabayashi et al., 1975), which also explains the observed reduction in defecation (Franco-Pons et al., 2007). On the other hand, diuresis was increased 10 fold, with urine having a decreased protein content and increased levels of Cu, Zn and MTs, indicative of an attempt at metal detoxification by MTs (Kang, 2006; Zatta et al., 2005).

Following CPZ intoxication, mice can display 'sickness behavior' which is characterized by weight loss, a general inactivity, lethargy, anhedonia, altered sleep and sexual patterns (De and Subramanian, 1982; Ludwin, 1978; Morell et al., 1998; Pattison and Jebbett, 1971; Petronilli and Zoratti, 1990; Stidworthy et al., 2003; Suzuki, 1969; Venturini, 1973). A hunched posture, catalepsy with the nose pushed into the bedding, a flaccid tail and gait abnormalities among which ataxia, hind limb paralysis and splayed hind limbs have also been noticed (Carey and Freeman, 1983; Franco-Pons et al., 2007; Hemm et al., 1971; Kesterson and Carlton, 1970, 1972; Love, 1988; Ludwin, 1978; Suzuki, 1969; Venturini, 1973; Wakabayashi et al., 1975). Following 3 weeks of CPZ treatment, mice display increased activity as observed by increased climbing behavior (Franco-Pons et al., 2007; Xu et al., 2009). The use of an adapted MOSS with a complex running wheel reveals motor skill dysfunction (impaired coordination of leg movement) as the CC becomes severely demyelinated during CPZ intoxication. Important to note is that this functional deficit only partially recovered during remyelination indicative of long lasting neurological deficits (Hibbits et al., 2009; Liebetanz and Merkler, 2006). Additionally, motor coordination impairment was also demonstrated using the rotarod and beam cross test (Franco-Pons et al., 2007; Hagemeyer et al., 2012).

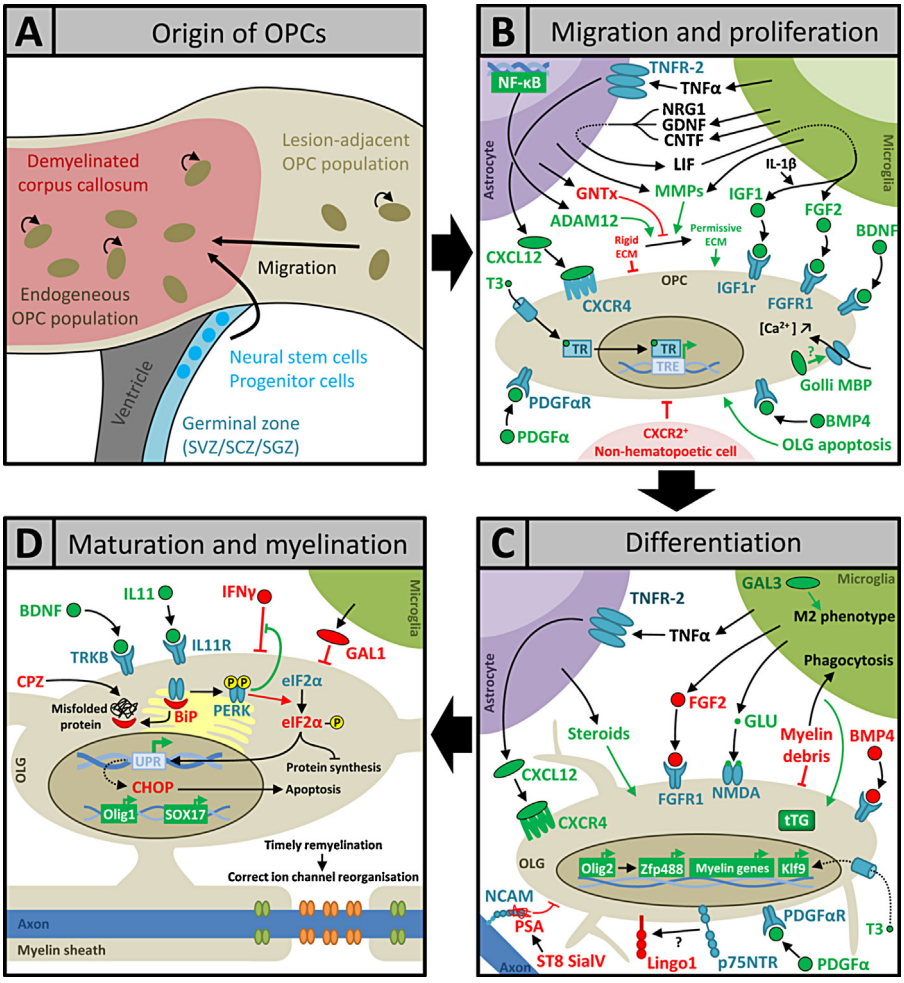

Fig. 5. Schematic overview of the spontaneous remyelination following CPZ-induced demyelination. Shown is the origin of the accumulating OPCs (A) and the factors influencing the different stages of remyelination: migration and proliferation (B), differentiation (C) and maturation and myelination (D). Depicted in green are factors which were shown to stimulate remyelination while factors in red were shown to inhibit remyelination.

7. Relevance as a model for human diseases

As described above, CPZ intoxication forms an excellent model to study pathology and/or therapy for human diseases, including MS, epilepsy and schizophrenia. Below we discuss the various similarities between CPZ induced CNS lesions and the observed pathologies in human diseases.

7.1. Cuprizone as a model for multiple sclerosis

Lucchinetti et al. (2000) published a key study describing 4 different lesion subtypes in MS. Pattern 1 and 2 lesions are thought to be autoimmune mediated, while both pattern 3 and 4 lesions were presumed to be a primary oligodendrogliapathy. Pattern 3 lesions in particular display many pathological similarities with CPZ-induced lesions: (i) actively demyelinating lesions with little involvement of T cells, but with the presence of many microglia/macrophages, (ii) hypoxia-like tissue injury with signs of metabolic stress and mitochondrial deficits, which eventually lead to pronounced OLG apoptosis as seen by an upregulation of p53, BCL-2 and FAS, as well as a nuclear translocation of AIF and PARP, (iii) MAG mRNA expression is downregulated before other myelin protein mRNA expression becomes downregulated, and (iv) ill-defined lesions borders that are not centered around a vein or venule (Aboul-Enein et al., 2003; Hesse et al., 2010; Li et al., 2008; Lucchinetti et al., 2000; Mahad et al., 2008; Veto et al., 2010). Much like the observed in pattern 3 MS lesions, CPZ treatment induces axonal swelling with hyperphosphorylated neurofilaments (SMI-32) and cytosolic translocation of HDAC1. This axonal swelling occurs due to a redistribution of Na^+ channels along the axon and mitochondrial deficits which cause a disturbance of Ca^{2+} and Na^+ homeostasis (Kim et al., 2010; Mahad et al., 2008). However, some differences were also noted as CPZ lesions do display a minimal presence of (non-contributing) $CD3^+$ T cells and no inflamed blood vessels, as compared to pattern 3 MS lesions (Kipp et al., 2009; Komoly, 2005; Liu et al., 2010a).

Motor related symptoms (fatigue, weakness, loss of sight, loss of balance and loss of speech, muscle spasms, bowel and bladder incontinence, ...), cognitive impairments (memory loss, anxiety, social deficits, ...) and even seizures have been observed in MS patients (Herring and Konradi, 2011). In the CPZ model, demyelination of the CC has been linked to impaired motor coordination between left and right paws (Liebetanz and Merkler, 2006). The degree of hippocampal lesions in MS correlates to cognitive dysfunction (especially long-term episodic memory) and severe demyelination of the hippocampal structure was observed after CPZ intoxication (Norkute et al., 2009). Demyelination of the basal ganglia has been linked to MS symptoms, such as fatigue, memory and motor skill impairment and extensive demyelination of the basal ganglia was also seen in the CPZ model (Pott et al., 2009).

Females were shown to be protected from MS attacks during pregnancy, but relapse rate increased significantly during the first

3 months post-partum, suggesting an important influence of sex steroids. In the CPZ model, estrogen was shown to be an important factor contributing to improved remyelination (Patel et al., 2013). Continuous estrogen administration for example was shown to prevent OLG apoptosis and delayed microglial accumulation and demyelination. (Taylor et al., 2010b). OLGs express estrogen receptor GPR30 and this receptor was shown to contribute to the positive effect of estrogen on remyelination following CPZ-induced demyelination (Hirahara et al., 2013). Males on the other hand are known to be less prone to develop MS and using the CPZ model it was shown that testosterone treatment promotes remyelination, even following chronic demyelination, and this effect was mediated via androgen receptor signaling (Hussain et al., 2013). While the CPZ model has shown the potential of estrogen and testosterone treatment to promote remyelination, and in contrast to human MS, no differences in de- and remyelination can be observed between male or female C57BL6/J mice following CPZ intoxication. CPZ was shown to disrupt the estrous cycle and to reduce the weight of male and female sex organs, which might affect sex hormone production (Taylor et al., 2010a). On a sidenote, gonadectomized female mice did show enhanced remyelination compared to gonadectomized male mice. As this difference only occurred following gonadectomy, this stresses the importance of intact sex hormone signaling and indicates a sex chromosome gene related effect on the remyelination process (Moore et al., 2013).

One of the biggest critics on the EAE model for human MS is that numerous developed therapeutics, which displayed beneficial effects in this model, are only of little (if any) benefit for the treatment of human MS, with TNFα being the textbook example. TNFα expression was found to correlate with MS severity, and inhibition of TNFα signaling ameliorated the EAE course (Klinkert et al., 1997; Martino et al., 1997). In contrast to the EAE model, anti TNFα treatment was found to worsen clinical MS symptoms in MS patients. Later on it was shown by Arnett et al. (2001) using the CPZ model, that TNFα displayed a dual role, where it was required for efficient remyelination. Other MS treatment examples are the administration of glucocorticoids or simvastatin and IFN-β treatment and these treatments are known to alleviate inflammation and reduce demyelination in MS. However, using the CPZ model, it was shown that these treatments have side-effects regarding remyelination which questions their long-term use as a possible MS treatment (Clarner et al., 2011; Miron et al., 2009; Schmidt et al., 2009; Trebst et al., 2007). Building upon these experiences, a recently published study investigated the in vivo efficacy of benztropine treatment, an M1 and/or M3 muscarinac receptor antagonist, using both the EAE model and the CPZ model. As such, the authors could clearly show that benztropine does not affect the immune response but rather stimulates remyelination in both in vivo mouse models (Deshmukh et al., 2013).

The above described examples are only a few of many studies using the CPZ model to test the efficacy of a certain compound or treatment in a non-immune mediated, primary oligodendropathy model. In addition, they substantiate the importance of remyelination as an important therapeutic goal in MS treatment. Administration of 0.2% CPZ for 12 weeks induces chronic lesions with limited or no remyelination. This failure to remyelinate (often while OPCs are still present) is regularly seen in MS as well. This control over the length of intoxication, and thus over remyelination, offers a major advantage over other MS models (Lucchinetti et al., 2000).

7.2. Cuprizone as a model for epilepsy

Epileptic seizures occur in about 3% of MS patients, but epilepsy itself is a striking neurodegenerative disease estimated to affect up to 50 million people worldwide. Similar to epilepsy, CPZ-treated mice display tonic-clonic seizures, loss of righting reflexes upon stress inducing stimuli, interictal spikes and frequent spike discharges but high amplitude discharges are rarely observed. While not completely resolved, possible explanations for the occurrence of seizures following CPZ treatment are: (i) a decrease in GABA, the increase in DOPA and the elevated GLU concentrations, ultimately leading to hyperstimulation, or (ii) demyelination of mossy neurons in the hippocampus leads to the loss of mossy neurons and thus to hyperexcitability of dentate granule cells (Hoffmann et al., 2008; Manrique-Hoyos et al., 2012).

7.3. Cuprizone as a model for schizophrenia

In humans, many cognitive functions like spatial working memory, social interactions, action planning, response inhibition, decision making and reward processing are mapped to the PFC and these functions appear altered in schizophrenia patients. As CPZ induces PFC demyelination, it has been used as a model for schizophrenia. However, it has to be noted that CPZ induces widespread demyelination, which does not happen in schizophrenia patients (Gregg et al., 2009; Makinodan et al., 2009; Xu et al., 2009–2011). Genetic studies in schizophrenia patients showed a down-regulation of genes related to OLGs, myelin and glial cells, while an up-regulation of stress related genes was found (Gregg et al., 2009). Multiple MRI studies also confirmed the involvement of white matter abnormalities in the PFC of schizophrenia patients (Xu et al., 2011).

Many of the behavioral alterations in schizophrenia patients were also found in CPZ treated mice. As such, it was shown that following CPZ treatment, mice have an impaired spatial memory (Makinodan et al., 2009; Xu et al., 2009–2011), a decreased thigmotaxis (Franco-Pons et al., 2007; Makinodan et al., 2009; Xu et al., 2011, 2009), sensorimotor gating deficits (Xu et al., 2010, 2009) and a decrease in social behavior like partner grooming, sniffing and mounting (Makinodan et al., 2009; Xu et al., 2009–2011). Concerning social behavior, a reduced CC size (as seen in the CPZ model) has been implicated with low sociability, possibly reflecting the social withdrawal as observed with schizophrenia patients.

Quetiapine (QUE), an antipsychotic drug commonly used to treat schizophrenia, prevents CPZ-induced white matter pathology and behavioral abnormalities as well as promotes remyelination. This substantiates the link between demyelination and behavioral abnormalities, and the importance of the CPZ model as a research model for schizophrenia (Chandran et al., 2011; Herring and Konradi, 2011; Xu et al., 2010; Zhang et al., 2008). Besides demyelination, other factors are inclined to play a role as not all behavior abnormalities recover during remyelination (Xu et al., 2011). Increased DA levels, reduced NE levels and inhibited MAO and DBH activities were found in the PFC after 2 to 3 weeks of CPZ treatment, but not after 6 weeks of CPZ treatment. This fits well within the dopamine hypothesis of schizophrenia, which attributes the observed gating deficits to disturbed dopamine signaling (Xu et al., 2010, 2009).

8. Concluding remarks

Ever since its conception, CPZ has been used to study de- and remyelination in rodents, despite its exact etiology remaining rather elusive. In this review, we first described two potential physico-chemical modi operandi. Although they appear contradictory, one does not (yet) exclude the other. However, regardless of its physico-chemical properties, CPZ reliably induces megamitochondria in OLGs, ultimately leading to OLG apoptosis. While it is generally accepted by most authors that CPZ-induced pathology originates from metabolic stress, we here summarized most

molecular, enzymatic and cellular alterations that result in the observed oxidative and metabolic stress. The following section covered the involvement of neutrophils, astrocytes and microglia to the initiation and progression of demyelination, but also the contribution of ongoing inflammatory reactions to remyelination processes. Although multiple molecular pathways involved during the observed inflammatory reactions are summarized in this manuscript, it is clear that further research will be necessary to fully understand the mechanism(s) behind CPZ-induced pathology. Full understanding of CPZ-induced pathology will be of utmost importance to claim the validity of novel MS, epilepsy or schizophrenia therapies developed into this model.

Acknowledgments

This work was prepared during the author's support by research grants G.0136.11 and G.0130.11 (granted to ZB, AvdL and PP) of the Fund for Scientific Research-Flanders (FWO-Vlaanderen, Belgium) and in part by funding received from the European Union's Seventh Framework Programme (FP7/2007-2013) under grant agreement no. 278850 (INMiND).

References

Aboul-Enein, F., Rauschka, H., Kornek, B., Stadelmann, C., Stefferl, A., Bruck, W., et al., 2003. Preferential loss of myelin-associated glycoprotein reflects hypoxia-like white matter damage in stroke and inflammatory brain diseases. J. Neuropathol. Exp. Neurol. 62, 25–33.

Acs, P., Kipp, M., Norkute, A., Johann, S., Clarner, T., Braun, A., et al., 2009. 17beta-estradiol and progesterone prevent cuprizone provoked demyelination of corpus callosum in male mice. Glia 57, 807–814.

Acs, P., Komoly, S., 2012. Selective ultrastructural vulnerability in the cuprizone-induced experimental demyelination. Ideggyogy Sz. 65, 266–270.

Acs, P., Selak, M.A., Komoly, S., Kalman, B., 2013. Distribution of oligodendrocyte loss and mitochondrial toxicity in the cuprizone-induced experimental demyelination model. J. Neuroimmunol. 262, 128–131.

Adamo, A.M., Paez, P.M., Escobar Cabrera, O.E., Wolfson, M., Franco, P.G., Pasquini, J.M., et al., 2006. Remyelination after cuprizone-induced demyelination in the rat is stimulated by apotransferrin. Exp. Neurol. 198, 519–529.

Arancibia-Carcamo, C.V., Osawa, H., Arnett, H.A., Haskova, Z., George, A.J., Ono, S.J., et al., 2004. A CIITA-independent pathway that promotes expression of endogenous rather than exogenous peptides in immune-privileged sites. Eur J. Immunol. 34, 471–480.

Armstrong, R.C., Le, T.Q., Flint, N.C., Vana, A.C., Zhou, Y.X., 2006. Endogenous cell repair of chronic demyelination. J. Neuropathol. Exp. Neurol. 65, 245–256.

Armstrong, R.C., Le, T.Q., Frost, E.E., Borke, R.C., Vana, A.C., 2002. Absence of fibroblast growth factor 2 promotes oligodendroglial repopulation of demyelinated white matter. J. Neurosci. 22, 8574–8585.

Arnett, H.A., Fancy, S.P., Alberta, J.A., Zhao, C., Plant, S.R., Kaing, S., et al., 2004. bHLH transcription factor Olig1 is required to repair demyelinated lesions in the CNS. Science 306, 2111–2115.

Arnett, H.A., Hellendall, R.P., Matsushima, G.K., Suzuki, K., Laubach, V.E., Sherman, P., et al., 2002. The protective role of nitric oxide in a neurotoxicant-induced demyelinating model. J. Immunol. 168, 427–433.

Arnett, H.A., Mason, J., Marino, M., Suzuki, K., Matsushima, G.K., Ting, J.P., 2001. TNF alpha promotes proliferation of oligodendrocyte progenitors and remyelination. Nat. Neurosci. 4, 1116–1122.

Arnett, H.A., Wang, Y., Matsushima, G.K., Suzuki, K., Ting, J.P., 2003. Functional genomic analysis of remyelination reveals importance of inflammation in oligodendrocyte regeneration. J. Neurosci. 23, 9824–9832.

Asano, M., Wakabayashi, T., Ishikawa, K., Kishimoto, H., 1978. Mechanism of the formation of megamitochondria by copper-chelating agents. IV. Role of fusion phenomenon in the cuprizone-induced megamitochondrial formation. Acta Pathol. Jpn. 28, 205–213.

Azami Tameh, A., Clarner, T., Beyer, C., Atlasi, M.A., Hassanzadeh, G., Naderian, H., 2013. Regional regulation of glutamate signaling during cuprizone-induced demyelination in the brain. Ann. Anat.—Anat. Anz. 195, 415–423.

Baertling, F., Kokozidou, M., Pufe, T., Clarner, T., Windoffer, R., Wruck, C.J., et al., 2010. ADAM12 is expressed by astrocytes during experimental demyelination. Brain Res. 1326, 1–14.

Bagchi, B., Al-Sabi, A., Kaza, S., Scholz, D., O'Leary, V.B., Dolly, J.O., et al., 2014. Disruption of myelin leads to ectopic expression of K(V)1.1 channels with abnormal conductivity of optic nerve axons in a cuprizone-induced model of demyelination. PLoS One 9, e87736.

Bak, L.K., Schousboe, A., Waagepetersen, H.S., 2006. The glutamate/GABA-glutamine cycle: aspects of transport, neurotransmitter homeostasis and ammonia transfer. J. Neurochem. 98, 641–653.

Bakker, D.A., Ludwin, S.K., 1987. Blood–brain barrier permeability during cuprizone-induced demyelination. Implications for the pathogenesis of immune-mediated demyelinating diseases. J. Neurol. Sci. 78, 125–137.

Bando, Y., Takakusaki, K., Ito, S., Terayama, R., Kashiwayanagi, M., Yoshida, S., 2008. Differential changes in axonal conduction following CNS demyelination in two mouse models. Eur. J. Neurosci. 28, 1731–1742.

Basoglu, H., Boylu, N.T., Kose, H., 2013. Cuprizone-induced demyelination in Wistar rats; electrophysiological and histological assessment. Eur. Rev. Med. Pharmacolo. Sci. 17, 2711–2717.

Baumann, N., Pham-Dinh, D., 2001. Biology of oligodendrocyte and myelin in the mammalian central nervous system. Physiol. Rev. 81, 871–927.

Bedard, A., Tremblay, P., Chernomoretz, A., Vallieres, L., 2007. Identification of genes preferentially expressed by microglia and upregulated during cuprizone-induced inflammation. Glia 55, 777–789.

Benardais, K., Kotsiari, A., Skuljec, J., Koutsoudaki, P.N., Gudi, V., Singh, V., et al., 2013. Cuprizone [bis(cyclohexylidenehydrazide)] is selectively toxic for mature oligodendrocytes. Neurotoxic. Res. 24, 244–250.

Benetti, F., Ventura, M., Salmini, B., Ceola, S., Carbonera, D., Mammi, S., et al., 2010. Cuprizone neurotoxicity, copper deficiency and neurodegeneration. Neurotoxicology 31, 509–517.

Bernard, F., Moreau-Fauvarque, C., Heitz-Marchaland, C., Zagar, Y., Dumas, L., Fouquet, S., et al., 2012. Role of transmembrane semaphorin Sema6A in oligodendrocyte differentiation and myelination. Glia 60, 1590–1604.

Bernardo, A., Greco, A., Levi, G., Minghetti, L., 2003. Differential lipid peroxidation, M_n superoxide, and bcl-2 expression contribute to the maturation-dependent vulnerability of oligodendrocytes to oxidative stress. J. Neuropathol. Exp. Neurol. 62, 509–519.

Biancotti, J.C., Kumar, S., de Vellis, J., 2008. Activation of inflammatory response by a combination of growth factors in cuprizone-induced demyelinated brain leads to myelin repair. Neurochem. Res. 33, 2615–2628.

Binder, M.D., Cate, H.S., Prieto, A.L., Kemper, D., Butzkueven, H., Gresle, M.M., et al., 2008. Gas6 deficiency increases oligodendrocyte loss and microglial activation in response to cuprizone-induced demyelination. J. Neurosci. 28, 5195–5206.

Binder, M.D., Xiao, J., Kemper, D., Ma, G.Z., Murray, S.S., Kilpatrick, T.J., 2011. Gas6 increases myelination by oligodendrocytes and its deficiency delays recovery following cuprizone-induced demyelination. PLoS One 6, e17727.

Blakemore, W.F., 1972. Observations on oligodendrocyte degeneration, the resolution of status spongiosus and remyelination in cuprizone intoxication in mice. J. Neurocytol. 1, 413–426.

Blakemore, W.F., 1973. Demyelination of the superior cerebellar peduncle in the mouse induced by cuprizone. J. Neurol. Sci. 20, 63–72.

Blakemore, W.F., 1984. The response of oligodendrocytes to chemical injury. Acta Neurol. Scand. Suppl. 100, 33–38.

Blakemore, W.F., Irvine, K.A., 2008. Endogenous or exogenous oligodendrocytes for remyelination. J. Neurol. Sci. 265, 43–46.

Briggs, D.T., Martin, C.B., Ingersoll, S.A., Barnum, S.R., Martin, B.K., 2007. Astrocyte-specific expression of a soluble form of the murine complement control protein Crry confers demyelination protection in the cuprizone model. Glia 55, 1405–1415.

Butts, B.D., Houde, C., Mehmet, H., 2008. Maturation-dependent sensitivity of oligodendrocyte lineage cells to apoptosis: implications for normal development and disease. Cell Death Differ. 15, 1178–1186.

Cammer, W., 1999. The neurotoxicant, cuprizone, retards the differentiation of oligodendrocytes in vitro. J. Neurol. Sci. 168, 116–120.

Cammer, W., Zhang, H., 1993. Atypical localization of the oligodendrocytic isoform (PI) of glutathione-*S*-transferase in astrocytes during cuprizone intoxication. J. Neurosci. Res. 36, 183–190.

Campbell, G.R., Mahad, D.J., 2011. Mitochondrial changes associated with demyelination: consequences for axonal integrity. Mitochondrion 12, 173–179.

Carey, E.M., Freeman, N.M., 1983. Biochemical changes in cuprizone-induced spongiform encephalopathy. I. Changes in the activities of 2′,3′-cyclic nucleotide 3′-phosphohydrolase, oligodendroglial ceramide galactosyl transferase, and the hydrolysis of the alkenyl group of alkenyl, acyl-glycerophospholipids by plasmalogenase in different regions of the brain. Neurochem. Res. 8, 1029–1044.

Carlton, W.W., 1966. Response of mice to the chelating agents sodium diethyldithiocarbamate, alpha-benzoinoxime, and biscyclohexanone oxaldihydrazone. Toxicol. Appl. Pharmacol. 8, 512–521.

Carlton, W.W., 1967. Studies on the induction of hydrocephalus and spongy degeneration by cuprizone feeding and attempts to antidote the toxicity. Life Sci. 6, 11–19.

Carlton, W.W., 1969. Spongiform encephalopathy induced in rats and guinea pigs by cuprizone. Exp. Mol. Pathol. 10, 274–287.

Cate, H.S., Sabo, J.K., Merlo, D., Kemper, D., Aumann, T.D., Robinson, J., et al., 2010a. Modulation of bone morphogenic protein signalling alters numbers of astrocytes and oligodendroglia in the subventricular zone during cuprizone-induced demyelination. J. Neurochem. 115, 11–22.

Cate, H.S., Wu, Q.Z., Kemper, D., Merlo, D., Wang, H.X., Fang, K., et al., 2010b. Influence of methylprednisolone on magnetic resonance and histological measures during cuprizone-induced demyelination. Neurosci. Lett. 483, 47–52.

Chandran, P., Upadhyay, J., Markosyan, S., Lisowski, A., Buck, W., Chin, C.L., et al., 2011. Magnetic resonance imaging and histological evidence for the blockade of cuprizone-induced demyelination in C57BL/6 mice. Neuroscience 202, 446–453.

Chen, L.P., Li, Z.F., Ping, M., Li, R., Liu, J., Xie, X.H., et al., 2012. Regulation of Olig2 during astroglial differentiation in the subventricular zone of a cuprizone-induced demyelination mouse model. Neuroscience 221, 96–107.

Chen, M.K., Baidoo, K., Verina, T., Guilarte, T.R., 2004. Peripheral benzodiazepine receptor imaging in CNS demyelination: functional implications of anatomical and cellular localization. Brain 127, 1379–1392.
Chen, M.K., Guilarte, T.R., 2006. Imaging the peripheral benzodiazepine receptor response in central nervous system demyelination and remyelination. Toxicol. Sci. 91, 532–539 (An Official Journal of the Society of Toxicology).
Clarner, T., Parabucki, A., Beyer, C., Kipp, M., 2011. Corticosteroids impair remyelination in the corpus callosum of cuprizone-treated mice. J. Neuroendocrinol. 23, 601–611.
Copray, J.C., Kust, B.M., Mantingh-Otter, I., Boddeke, H.W., 2005. p75NTR independent oligodendrocyte death in cuprizone-induced demyelination in C57BL/6 mice. Neuropathol. Appl. Neurobiol. 31, 600–609.
Crawford, D.K., Mangiardi, M., Xia, X., Lopez-Valdes, H.E., Tiwari-Woodruff, S.K., 2009. Functional recovery of callosal axons following demyelination: a critical window. Neuroscience 164, 1407–1421.
De, A.K., Subramanian, M., 1982. Effect of cuprizone feeding on hepatic superoxide dismutase and cytochrome oxidase activities in mice. Experientia 38, 784–785.
Deshmukh, V.A., Tardif, V., Lyssiotis, C.A., Green, C.C., Kerman, B., Kim, H.J., et al., 2013. A regenerative approach to the treatment of multiple sclerosis. Nature 502, 327–332.
Dewar, D., Underhill, S.M., Goldberg, M.P., 2003. Oligodendrocytes and ischemic brain injury. J. Cereb. Blood Flow Metab. 23, 263–274.
Doan, V., Kleindienst, A.M., McMahon, E.J., Long, B.R., Matsushima, G.K., Taylor, L.C., 2013. Abbreviated exposure to cuprizone is sufficient to induce demyelination and oligodendrocyte loss. J. Neurosci. Res. 91, 363–373.
Dugas, J.C., Ibrahim, A., Barres, B.A., 2012. The T3-induced gene KLF9 regulates oligodendrocyte differentiation and myelin regeneration. Mol. Cell. Neurosci. 50, 45–57.
Dupree, J.L., Mason, J.L., Marcus, J.R., Stull, M., Levinson, R., Matsushima, G.K., et al., 2004. Oligodendrocytes assist in the maintenance of sodium channel clusters independent of the myelin sheath. Neuron Glia Biol. 1, 179–192.
Dutta, R., Chomyk, A.M., Chang, A., Ribaudo, M.V., Deckard, S.A., Doud, M.K., et al., 2013. Hippocampal demyelination and memory dysfunction are associated with increased levels of the neuronal microRNA miR-124 and reduced AMPA receptors. Ann. Neurol. 73, 637–645.
Elsworth, S., Howell, J.M., 1973. Variation in the response of mice to cuprizone. Res. Vet. Sci. 14, 385–387.
Emery, B., Cate, H.S., Marriott, M., Merson, T., Binder, M.D., Snell, C., et al., 2006. Suppressor of cytokine signaling 3 limits protection of leukemia inhibitory factor receptor signaling against central demyelination. Proc. Natl. Acad. Sci. U.S.A. 103, 7859–7864.
Fairless, A.H., Dow, H.C., Toledo, M.M., Malkus, K.A., Edelmann, M., Li, H., et al., 2008. Low sociability is associated with reduced size of the corpus callosum in the BALB/cJ inbred mouse strain. Brain Res. 1230, 211–217.
Farooqui, A.A., Horrocks, L.A., 2001. Plasmalogens: workhorse lipids of membranes in normal and injured neurons and glia. Neuroscientist 7, 232–245 (A Review Journal Bringing Neurobiology Neurology and Psychiatry).
Flatmark, T., Kryvi, H., Tangeras, A., 1980. Induction of megamitochondria by cuprizone(biscyclohexanone oxaldihydrazone), Evidence for an inhibition of the mitochondrial division process. Eur. J. Cell Biol. 23, 141–148.
Franco-Pons, N., Torrente, M., Colomina, M.T., Vilella, E., 2007. Behavioral deficits in the cuprizone-induced murine model of demyelination/remyelination. Toxicol. Lett. 169, 205–213.
Franco, P.G., Silvestroff, L., Soto, E.F., Pasquini, J.M., 2008. Thyroid hormones promote differentiation of oligodendrocyte progenitor cells and improve remyelination after cuprizone-induced demyelination. Exp. Neurol. 212, 458–467.
Gao, X., Gillig, T.A., Ye, P., D'Ercole, A.J., Matsushima, G.K., Popko, B., 2000. Interferon-gamma protects against cuprizone-induced demyelination. Mol. Cell. Neurosci. 16, 338–349.
Geva, M., Cabilly, Y., Assaf, Y., Mindroul, N., Marom, L., Raini, G., et al., 2010. A mouse model for eukaryotic translation initiation factor 2B-leucodystrophy reveals abnormal development of brain white matter. Brain 133, 2448–2461.
Goldberg, J., Daniel, M., van Heuvel, Y., Victor, M., Beyer, C., Clarner, T., et al., 2013. Short-term cuprizone feeding induces selective amino acid deprivation with concomitant activation of an integrated stress response in oligodendrocytes. Cell. Mol. Neurobiol. 33, 1087–1098.
Gregg, J.R., Herring, N.R., Naydenov, A.V., Hanlin, R.P., Konradi, C., 2009. Downregulation of oligodendrocyte transcripts is associated with impaired prefrontal cortex function in rats. Schizophr. Res. 113, 277–287.
Gudi, V., Moharregh-Khiabani, D., Skripuletz, T., Koutsoudaki, P.N., Kotsiari, A., Skuljec, J., et al., 2009. Regional differences between grey and white matter in cuprizone induced demyelination. Brain Res. 1283, 127–138.
Gudi, V., Skuljec, J., Yildiz, O., Frichert, K., Skripuletz, T., Moharregh-Khiabani, D., et al., 2011. Spatial and temporal profiles of growth factor expression during CNS demyelination reveal the dynamics of repair priming. PLoS One 6, e22623.
Guglielmetti, C., Praet, J., Rangarajan, J.R., Vreys, R., De Vocht, N., Maes, F., et al., 2013. Multimodal imaging of subventricular zone neural stem/progenitor cells in the cuprizone mouse model reveals increased neurogenic potential for the olfactory bulb pathway, but no contribution to remyelination of the corpus callosum. NeuroImage 86, 99–110.
Hagemeier, K., Lurbke, A., Hucke, S., Albrecht, S., Preisner, A., Klassen, E., et al., 2013. Puma, but not noxa is essential for oligodendroglial cell death. Glia 61, 1712–1723.
Hagemeyer, N., Boretius, S., Ott, C., Von Streitberg, A., Welpinghus, H., Sperling, S., et al., 2012. Erythropoietin attenuates neurological and histological consequences of toxic demyelination in mice. Mol. Med. 18, 628–635.
Harsan, L.A., Steibel, J., Zaremba, A., Agin, A., Sapin, R., Poulet, P., et al., 2008. Recovery from chronic demyelination by thyroid hormone therapy: myelinogenesis induction and assessment by diffusion tensor magnetic resonance imaging. J. Neurosci. 28, 14189–14201.
Hemdan, S., Almazan, G., 2006. Iron contributes to dopamine-induced toxicity in oligodendrocyte progenitors. Neuropathol. Appl. Neurobiol. 32, 428–440.
Hemm, R.D., Carlton, W.W., Welser, J.R., 1971. Ultrastructural changes of cuprizone encephalopathy in mice. Toxicol. Appl. Pharmacol. 18, 869–882.
Hermida-Ameijeiras, A., Mendez-Alvarez, E., Sanchez-Iglesias, S., Sanmartin-Suarez, C., Soto-Otero, R., 2004. Autoxidation and MAO-mediated metabolism of dopamine as a potential cause of oxidative stress: role of ferrous and ferric ions. Neurochem. Int. 45, 103–116.
Herring, N.R., Konradi, C., 2011. Myelin, copper, and the cuprizone model of schizophrenia. Front. Biosci. (Schol Ed) 3, 23–40.
Hesse, A., Wagner, M., Held, J., Bruck, W., Salinas-Riester, G., Hao, Z., et al., 2010. In toxic demyelination oligodendroglial cell death occurs early and is FAS independent. Neurobiol. Dis. 37, 362–369.
Hibbits, N., Pannu, R., Wu, T.J., Armstrong, R.C., 2009. Cuprizone demyelination of the corpus callosum in mice correlates with altered social interaction and impaired bilateral sensorimotor coordination. ASN Neuro 1, e00013.
Hibbits, N., Yoshino, J., Le, T.Q., Armstrong, R.C., 2012. Astrogliosis during acute and chronic cuprizone demyelination and implications for remyelination. ASN Neuro 4, 393–408.
Hider, R.C., Ma, Y., Molina-Holgado, F., Gaeta, A., Roy, S., 2008. Iron chelation as a potential therapy for neurodegenerative disease. Biochem. Soc. Trans. 36, 1304–1308.
Hirahara, Y., Matsuda, K.I., Yamada, H., Saitou, A., Morisaki, S., Takanami, K., et al., 2013. G protein-coupled receptor 30 contributes to improved remyelination after cuprizone-induced demyelination. Glia 61, 420–431.
Hiremath, M.M., Chen, V.S., Suzuki, K., Ting, J.P., Matsushima, G.K., 2008. MHC class II exacerbates demyelination in vivo independently of T cells. J. Neuroimmunol. 203, 23–32.
Hiremath, M.M., Saito, Y., Knapp, G.W., Ting, J.P., Suzuki, K., Matsushima, G.K., 1998. Microglial/macrophage accumulation during cuprizone-induced demyelination in C57BL/6 mice. J. Neuroimmunol. 92, 38–49.
Hoehn, H.J., Kress, Y., Sohn, A., Brosnan, C.F., Bourdon, S., Shafit-Zagardo, B., 2008. $Axl^{-/-}$ mice have delayed recovery and prolonged axonal damage following cuprizone toxicity. Brain Res. 1240, 1–11.
Hoffmann, K., Lindner, M., Groticke, I., Stangel, M., Loscher, W., 2008. Epileptic seizures and hippocampal damage after cuprizone-induced demyelination in C57BL/6 mice. Exp. Neurol. 210, 308–321.
Horiuchi, M., Wakayama, K., Itoh, A., Kawai, K., Pleasure, D., Ozato, K., et al., 2012. Interferon regulatory factor 8/interferon consensus sequence binding protein is a critical transcription factor for the physiological phenotype of microglia. J. Neuroinflammation 9, 227.
Hoyos, H.C., Rinaldi, M., Mendez-Huergo, S.P., Marder, M., Rabinovich, G.A., Pasquini, J.M., et al., 2014. Galectin-3 controls the response of microglial cells to limit cuprizone-induced demyelination. Neurobiol. Dis. 62, 441–455.
Hu, Y., Lee, X., Ji, B., Guckian, K., Apicco, D., Pepinsky, R.B., et al., 2011. Sphingosine 1-phosphate receptor modulator fingolimod (FTY720) does not promote remyelination in vivo. Mol. Cell. Neurosci. 48, 72–81.
Hussain, R., Ghoumari, A.M., Bielecki, B., Steibel, J., Boehm, N., Liere, P., et al., 2013. The neural androgen receptor: a therapeutic target for myelin repair in chronic demyelination. Brain 136, 132–146.
Ingersoll, S.A., Martin, C.B., Barnum, S.R., Martin, B.K., 2010. CNS-specific expression of C3a and C5a exacerbate demyelination severity in the cuprizone model. Mol. Immunol. 48, 219–230.
Iocca, H.A., Plant, S.R., Wang, Y., Runkel, L., O'Connor, B.P., Lundsmith, E.T., et al., 2008. TNF superfamily member TWEAK exacerbates inflammation and demyelination in the cuprizone-induced model. J. Neuroimmunol. 194, 97–106.
Irvine, K.A., Blakemore, W.F., 2006. Age increases axon loss associated with primary demyelination in cuprizone-induced demyelination in C57BL/6 mice. J. Neuroimmunol. 175, 69–76.
Irvine, K.A., Blakemore, W.F., 2008. Remyelination protects axons from demyelination-associated axon degeneration. Brain 131, 1464–1477.
Islam, M.S., Tatsumi, K., Okuda, H., Shiosaka, S., Wanaka, A., 2009. Olig2-expressing progenitor cells preferentially differentiate into oligodendrocytes in cuprizone-induced demyelinated lesions. Neurochem. Int. 54, 192–198.
Jha, S., Srivastava, S.Y., Brickey, W.J., Iocca, H., Toews, A., Morrison, J.P., et al., 2010. The inflammasome sensor, NLRP3, regulates CNS inflammation and demyelination via caspase-1 and interleukin-18. J. Neurosci. 30, 15811–15820.
Jurevics, H., Hostettler, J., Muse, E.D., Sammond, D.W., Matsushima, G.K., Toews, A.D., et al., 2001. Cerebroside synthesis as a measure of the rate of remyelination following cuprizone-induced demyelination in brain. J. Neurochem. 77, 1067–1076.
Jurevics, H., Largent, C., Hostettler, J., Sammond, D.W., Matsushima, G.K., Kleindienst, A., et al., 2002. Alterations in metabolism and gene expression in brain regions during cuprizone-induced demyelination and remyelination. J. Neurochem. 82, 126–136.
Juurlink, B.H., Thorburne, S.K., Hertz, L., 1998. Peroxide-scavenging deficit underlies oligodendrocyte susceptibility to oxidative stress. Glia 22, 371–378.
Kanekiyo, K., Inamori, K., Kitazume, S., Sato, K., Maeda, J., Higuchi, M., et al., 2013. Loss of branched *O*-mannosyl glycans in astrocytes accelerates remyelination. J. Neurosci. 33, 10037–10047.
Kang, Y.J., 2006. Metallothionein redox cycle and function. Exp. Biol. Med. (Maywood) 231, 1459–1467.

Kang, Z., Liu, L., Spangler, R., Spear, C., Wang, C., Gulen, M.F., et al., 2012. IL-17-induced Act1-mediated signaling is critical for cuprizone-induced demyelination. J. Neurosci. 32, 8284–8292.
Kanno, T., Sasaki, S., Yamada, N., Kawasako, K., Tsuchitani, M., 2012. Hexachlorophene and cuprizone induce the spongy change of the developing rat brain by different mechanisms: the role of 2′,3′-cyclic nucleotide 3′-phosphodiesterase (CNPase). J. Vet. Med. Sci. 74, 837–843 (the Japanese Society of Veterinary Science).
Kesterson, J.W., Carlton, W.W., 1970. Aqueductal stenosis as the cause of hydrocephalus in mice fed the substituted hydrazine, cuprizone. Exp. Mol. Pathol. 13, 281–294.
Kesterson, J.W., Carlton, W.W., 1971. Histopathologic and enzyme histochemical observations of the cuprizone-induced brain edema. Exp. Mol. Pathol. 15, 82–96.
Kesterson, J.W., Carlton, W.W., 1972. Cuprizone toxicosis in mice—attempts to antidote the toxicity. Toxicol. Appl. Pharmacol. 22, 6–13.
Kim, H.J., Miron, V.E., Dukala, D., Proia, R.L., Ludwin, S.K., Traka, M., et al., 2011. Neurobiological effects of sphingosine 1-phosphate receptor modulation in the cuprizone model. FASEB J. 25, 1509–1518 (Official Publication of the Federation of American Societies for Experimental Biology).
Kim, J.Y., Shen, S., Dietz, K., He, Y., Howell, O., Reynolds, R., et al., 2010. HDAC1 nuclear export induced by pathological conditions is essential for the onset of axonal damage. Nat. Neurosci. 13, 180–189.
Kim, S., Steelman, A.J., Zhang, Y., Kinney, H.C., Li, J., 2012. Aberrant upregulation of astroglial ceramide potentiates oligodendrocyte injury. Brain Pathol. 22, 41–57.
Kimberlin, R.H., Collis, S.C., Walker, C.A., 1976. Profiles of brain glycosidase activity in cuprizone-fed Syrian hamsters and in scrapie-affected mice, rats, Chinese hamsters and Syrian hamsters. J. Comp. Pathol. 86, 135–142.
Kipp, M., Clarner, T., Dang, J., Copray, S., Beyer, C., 2009. The cuprizone animal model: new insights into an old story. Acta Neuropathol. 118, 723–736.
Kipp, M., Gingele, S., Pott, F., Clarner, T., van der Valk, P., Denecke, B., et al., 2011. BLBP-expression in astrocytes during experimental demyelination and in human multiple sclerosis lesions. Brain Behav. Immun. 25, 1554–1568.
Klinkert, W.E., Kojima, K., Lesslauer, W., Rinner, W., Lassmann, H., Wekerle, H., 1997. TNF-alpha receptor fusion protein prevents experimental auto-immune encephalomyelitis and demyelination in Lewis rats: an overview. J. Neuroimmunol. 72, 163–168.
Komoly, S., 2005. Experimental demyelination caused by primary oligodendrocyte dystrophy. Regional distribution of the lesions in the nervous system of mice [corrected]. Ideggyogy. Sz. 58, 40–43.
Komoly, S., Hudson, L.D., Webster, H.D., Bondy, C.A., 1992. Insulin-like growth factor I gene expression is induced in astrocytes during experimental demyelination. Proc. Natl. Acad. Sci. U.S.A. 89, 1894–1898.
Konig, R., Stillfried, M., Aperdannier, P., Clarner, T., Beyer, C., Kipp, M., et al., 2012. Expression of retinoid X receptor beta is induced in astrocytes during corpus callosum demyelination. J. Chem. Neuroanat. 43, 120–132.
Kotter, M.R., Li, W.W., Zhao, C., Franklin, R.J., 2006. Myelin impairs CNS remyelination by inhibiting oligodendrocyte precursor cell differentiation. J. Neurosci. 26, 328–332.
Koutsoudaki, P.N., Hildebrandt, H., Gudi, V., Skripuletz, T., Skuljec, J., Stangel, M., 2010. Remyelination after cuprizone induced demyelination is accelerated in mice deficient in the polysialic acid synthesizing enzyme St8siaIV. Neuroscience 171, 235–244.
Kumar, S., Biancotti, J.C., Yamaguchi, M., de Vellis, J., 2007. Combination of growth factors enhances remyelination in a cuprizone-induced demyelination mouse model. Neurochem. Res. 32, 783–797.
Lee, K.K., de Repentigny, Y., Saulnier, R., Rippstein, P., Macklin, W.B., Kothary, R., 2006. Dominant-negative beta1 integrin mice have region-specific myelin defects accompanied by alterations in MAPK activity. Glia 53, 836–844.
Li, C., Xiao, L., Liu, X., Yang, W., Shen, W., Hu, C., et al., 2013a. A functional role of NMDA receptor in regulating the differentiation of oligodendrocyte precursor cells and remyelination. Glia 61, 732–749.
Li, J., Ghiani, C.A., Kim, J.Y., Liu, A., Sandoval, J., DeVellis, J., et al., 2008. Inhibition of p53 transcriptional activity: a potential target for future development of therapeutic strategies for primary demyelination. J. Neurosci. 28, 6118–6127.
Li, Y., Zhang, Y., Han, W., Hu, F., Qian, Y., Chen, Q., 2013b. TRO19622 promotes myelin repair in a rat model of demyelination. Int. J. Neurosci. 123, 810–822.
Liberto, C.M., Albrecht, P.J., Herx, L.M., Yong, V.W., Levison, S.W., 2004. Pro-regenerative properties of cytokine-activated astrocytes. J. Neurochem. 89, 1092–1100.
Liebetanz, D., Merkler, D., 2006. Effects of commissural de- and remyelination on motor skill behaviour in the cuprizone mouse model of multiple sclerosis. Exp. Neurol. 202, 217–224.
Lin, W., Kemper, A., Dupree, J.L., Harding, H.P., Ron, D., Popko, B., 2006. Interferon-gamma inhibits central nervous system remyelination through a process modulated by endoplasmic reticulum stress. Brain 129, 1306–1318.
Lin, Y., Huang, G., Jamison, S., Li, J., Harding, H.P., Ron, D., et al., 2014. PERK activation preserves the viability and function of remyelinating oligodendrocytes in immune-mediated demyelinating diseases. Am. J. Pathol. 184, 507–519.
Linares, D., Taconis, M., Mana, P., Correcha, M., Fordham, S., Staykova, M., et al., 2006. Neuronal nitric oxide synthase plays a key role in CNS demyelination. J. Neurosci. 26, 12672–12681.
Lindner, M., Trebst, C., Heine, S., Skripuletz, T., Koutsoudaki, P.N., Stangel, M., 2008. The chemokine receptor CXCR2 is differentially regulated on glial cells in vivo but is not required for successful remyelination after cuprizone-induced demyelination. Glia 56, 1104–1113.
Liu, L., Belkadi, A., Darnall, L., Hu, T., Drescher, C., Cotleur, A.C., et al., 2010a. CXCR2-positive neutrophils are essential for cuprizone-induced demyelination: relevance to multiple sclerosis. Nat. Neurosci. 13, 319–326.
Liu, L., Darnall, L., Hu, T., Choi, K., Lane, T.E., Ransohoff, R.M., 2010b. Myelin repair is accelerated by inactivating CXCR2 on nonhematopoietic cells. J. Neurosci. 30, 9074–9083.
Ljutakova, S.G., Russanov, E.M., 1985. Differences in the in vivo effects of cuprizone on superoxide dismutase activity in rat liver cytosol and mitochondrial intermembrane space. Acta Physiol. Pharmacol. Bulg. 11, 56–61.
Love, S., 1988. Cuprizone neurotoxicity in the rat: morphologic observations. J. Neurol. Sci. 84, 223–237.
Lu, B., Pang, P.T., Woo, N.H., 2005. The yin and yang of neurotrophin action. Nat. Rev. Neurosci. 6, 603–614.
Lucchinetti, C., Bruck, W., Parisi, J., Scheithauer, B., Rodriguez, M., Lassmann, H., 2000. Heterogeneity of multiple sclerosis lesions: implications for the pathogenesis of demyelination. Ann. Neurol. 47, 707–717.
Ludwin, S.K., 1978. Central nervous system demyelination and remyelination in the mouse: an ultrastructural study of cuprizone toxicity. Lab. Invest. 39, 597–612.
Ludwin, S.K., 1980. Chronic demyelination inhibits remyelination in the central nervous system. An analysis of contributing factors. Lab. Invest. 43, 382–387.
Ludwin, S.K., Sternberger, N.H., 1984. An immunohistochemical study of myelin proteins during remyelination in the central nervous system. Acta Neuropathol. 63, 240–248.
Mahad, D., Ziabreva, I., Lassmann, H., Turnbull, D., 2008. Mitochondrial defects in acute multiple sclerosis lesions. Brain 131, 1722–1735.
Maheshwari, A., Janssens, K., Bogie, J., Van Den Haute, C., Struys, T., Lambrichts, I., et al., 2013. Local overexpression of interleukin-11 in the central nervous system limits demyelination and enhances remyelination. Mediators Inflammation 2013, 685317.
Makinodan, M., Yamauchi, T., Tatsumi, K., Okuda, H., Takeda, T., Kiuchi, K., et al., 2009. Demyelination in the juvenile period, but not in adulthood, leads to long-lasting cognitive impairment and deficient social interaction in mice. Prog. Neuropsychopharmacol. Biol. Psychiatry 33, 978–985.
Malhotra, J.D., Kaufman, R.J., 2007. Endoplasmic reticulum stress and oxidative stress: a vicious cycle or a double-edged sword? Antioxid. Redox Signal. 9, 2277–2293.
Mana, P., Fordham, S.A., Staykova, M.A., Correcha, M., Silva, D., Willenborg, D.O., et al., 2009. Demyelination caused by the copper chelator cuprizone halts T cell mediated autoimmune neuroinflammation. J. Neuroimmunol. 210, 13–21.
Mana, P., Linares, D., Fordham, S., Staykova, M., Willenborg, D., 2006. Deleterious role of IFNgamma in a toxic model of central nervous system demyelination. Am. J. Pathol. 168, 1464–1473.
Manrique-Hoyos, N., Jurgens, T., Gronborg, M., Kreutzfeldt, M., Schedensack, M., Kuhlmann, T., et al., 2012. Late motor decline after accomplished remyelination: impact for progressive multiple sclerosis. Ann. Neurol. 71, 227–244.
Marrif, H., Juurlink, B.H.J., 2003. Differential vulnerability of oligodendrocytes and astrocytes to hypoxic–ischemic stresses. Advances in Molecular and Cell Biology 31, 857–867, Elsevier.
Marriott, M.P., Emery, B., Cate, H.S., Binder, M.D., Kemper, D., Wu, Q., et al., 2008. Leukemia inhibitory factor signaling modulates both central nervous system demyelination and myelin repair. Glia 56, 686–698.
Martino, G., Consiglio, A., Franciotta, D.M., Corti, A., Filippi, M., Vandenbroeck, K., et al., 1997. Tumor necrosis factor alpha and its receptors in relapsing-remitting multiple sclerosis. J. Neurol. Sci. 152, 51–61.
Mason, J.L., Jones, J.J., Taniike, M., Morell, P., Suzuki, K., Matsushima, G.K., 2000a. Mature oligodendrocyte apoptosis precedes IGF-1 production and oligodendrocyte progenitor accumulation and differentiation during demyelination/remyelination. J. Neurosci. Res. 61, 251–262.
Mason, J.L., Langaman, C., Morell, P., Suzuki, K., Matsushima, G.K., 2001a. Episodic demyelination and subsequent remyelination within the murine central nervous system: changes in axonal calibre. Neuropathol. Appl. Neurobiol. 27, 50–58.
Mason, J.L., Suzuki, K., Chaplin, D.D., Matsushima, G.K., 2001b. Interleukin-1beta promotes repair of the CNS. J. Neurosci. 21, 7046–7052.
Mason, J.L., Toews, A., Hostettler, J.D., Morell, P., Suzuki, K., Goldman, J.E., et al., 2004. Oligodendrocytes and progenitors become progressively depleted within chronically demyelinated lesions. Am. J. Pathol. 164, 1673–1682.
Mason, J.L., Ye, P., Suzuki, K., D'Ercole, A.J., Matsushima, G.K., 2000b. Insulin-like growth factor-1 inhibits mature oligodendrocyte apoptosis during primary demyelination. J. Neurosci. 20, 5703–5708.
Matsushima, G.K., Morell, P., 2001. The neurotoxicant, cuprizone, as a model to study demyelination and remyelination in the central nervous system. Brain Pathol. 11, 107–116.
Mattner, F., Bandin, D.L., Staykova, M., Berghofer, P., Gregoire, M.C., Ballantyne, P., et al., 2011. Evaluation of [(1)(2)(3)I]-CLINDE as a potent SPECT radiotracer to assess the degree of astroglia activation in cuprizone-induced neuroinflammation. Eur. J. Nucl. Med. Mol. Imaging 38, 1516–1528.
McMahon, E.J., Cook, D.N., Suzuki, K., Matsushima, G.K., 2001. Absence of macrophage-inflammatory protein-1alpha delays central nervous system demyelination in the presence of an intact blood-brain barrier. J. Immunol. 167, 2964–2971.
McMahon, E.J., Suzuki, K., Matsushima, G.K., 2002. Peripheral macrophage recruitment in cuprizone-induced CNS demyelination despite an intact blood-brain barrier. J. Neuroimmunol. 130, 32–45.
Merkler, D., Boretius, S., Stadelmann, C., Ernsting, T., Michaelis, T., Frahm, J., et al., 2005. Multicontrast MRI of remyelination in the central nervous system. NMR Biomed. 18, 395–403.

Messori, L., Casini, A., Gabbiani, C., Sorace, L., Muniz-Miranda, M., Zatta, P., 2007. Unravelling the chemical nature of copper cuprizone. Dalton Trans. (21), 2112–2114.
Mi, S., Miller, R.H., Tang, W., Lee, X., Hu, B., Wu, W., et al., 2009. Promotion of central nervous system remyelination by induced differentiation of oligodendrocyte precursor cells. Ann. Neurol. 65, 304–315.
Mierzwa, A.J., Zhou, Y.X., Hibbits, N., Vana, A.C., Armstrong, R.C., 2013. FGF2 and FGFR1 signaling regulate functional recovery following cuprizone demyelination. Neurosci. Lett. 548, 280–285.
Millet, V., Marder, M., Pasquini, L.A., 2012. Adult CNP::EGFP transgenic mouse shows pronounced hypomyelination and an increased vulnerability to cuprizone-induced demyelination. Exp. Neurol. 233, 490–504.
Millet, V., Moiola, C.P., Pasquini, J.M., Soto, E.F., Pasquini, L.A., 2009. Partial inhibition of proteasome activity enhances remyelination after cuprizone-induced demyelination. Exp. Neurol. 217, 282–296.
Miron, V.E., Zehntner, S.P., Kuhlmann, T., Ludwin, S.K., Owens, T., Kennedy, T.E., et al., 2009. Statin therapy inhibits remyelination in the central nervous system. Am. J. Pathol. 174, 1880–1890.
Miwa, S., Lawless, C., von Zglinicki, T., 2008. Mitochondrial turnover in liver is fast in vivo and is accelerated by dietary restriction: application of a simple dynamic model. Aging cell 7, 920–923.
Moll, N.M., Hong, E., Fauveau, M., Naruse, M., Kerninon, C., Tepavcevic, V., et al., 2013. SOX17 is expressed in regenerating oligodendrocytes in experimental models of demyelination and in multiple sclerosis. Glia 61, 1659–1672.
Moore, S., Patel, R., Hannsun, G., Yang, J., Tiwari-Woodruff, S.K., 2013. Sex chromosome complement influences functional callosal myelination. Neuroscience 245, 166–178.
Morell, P., Barrett, C.V., Mason, J.L., Toews, A.D., Hostettler, J.D., Knapp, G.W., et al., 1998. Gene expression in brain during cuprizone-induced demyelination and remyelination. Mol. Cell. Neurosci. 12, 220–227.
Murtie, J.C., Zhou, Y.X., Le, T.Q., Vana, A.C., Armstrong, R.C., 2005. PDGF and FGF2 pathways regulate distinct oligodendrocyte lineage responses in experimental demyelination with spontaneous remyelination. Neurobiol. Dis. 19, 171–182.
Nelecz, M.J., Wroniszewska, A., Famulski, K.S., Wojtczak, L., 1982. Changes in the mitochondrial surface potential during cuprizone-induced formation of megamitochondria. Eur. J. Cell Biol. 27, 289–295.
Neumann, H., Kotter, M.R., Franklin, R.J., 2009. Debris clearance by microglia: an essential link between degeneration and regeneration. Brain 132, 288–295.
Nilsson, G., 1950. A new colour reaction on copper and ceratin carbonyl compounds. Acta Chem. Scand. 4, 205–208.
Norkute, A., Hieble, A., Braun, A., Johann, S., Clarner, T., Baumgartner, W., et al., 2009. Cuprizone treatment induces demyelination and astrocytosis in the mouse hippocampus. J. Neurosci. Res. 87, 1343–1355.
Olah, M., Amor, S., Brouwer, N., Vinet, J., Eggen, B., Biber, K., et al., 2012. Identification of a microglia phenotype supportive of remyelination. Glia 60, 306–321.
Othman, A., Frim, D.M., Polak, P., Vujicic, S., Arnason, B.G., Boullerne, A.I., 2011. Olig1 is expressed in human oligodendrocytes during maturation and regeneration. Glia 59, 914–926.
Paez, P.M., Cheli, V.T., Ghiani, C.A., Spreuer, V., Handley, V.W., Campagnoni, A.T., 2012. Golli myelin basic proteins stimulate oligodendrocyte progenitor cell proliferation and differentiation in remyelinating adult mouse brain. Glia 60, 1078–1093.
Palumbo, S., Toscano, C.D., Parente, L., Weigert, R., Bosetti, F., 2011a. The cyclooxygenase-2 pathway via the PGE(2) EP2 receptor contributes to oligodendrocytes apoptosis in cuprizone-induced demyelination. J. Neurochem. 121, 418–427.
Palumbo, S., Toscano, C.D., Parente, L., Weigert, R., Bosetti, F., 2011b. Time-dependent changes in the brain arachidonic acid cascade during cuprizone-induced demyelination and remyelination. Prostaglandins Leukot. Essent. Fatty Acids 85, 29–35.
Parenti, R., Cicirata, F., Zappala, A., Catania, A., La Delia, F., Cicirata, V., et al., 2010. Dynamic expression of Cx47 in mouse brain development and in the cuprizone model of myelin plasticity. Glia 58, 1594–1609.
Pasquini, L.A., Calatayud, C.A., Bertone Una, A.L., Millet, V., Pasquini, J.M., Soto, E.F., 2007. The neurotoxic effect of cuprizone on oligodendrocytes depends on the presence of pro-inflammatory cytokines secreted by microglia. Neurochem. Res. 32, 279–292.
Pasquini, L.A., Millet, V., Hoyos, H.C., Giannoni, J.P., Croci, D.O., Marder, M., et al., 2011. Galectin-3 drives oligodendrocyte differentiation to control myelin integrity and function. Cell Death Differ. 18, 1746–1756.
Pasquini, L.A., Paez, P.M., Moreno, M.A., Pasquini, J.M., Soto, E.F., 2003. Inhibition of the proteasome by lactacystin enhances oligodendroglial cell differentiation. J. Neurosci. 23, 4635–4644.
Patel, J.R., McCandless, E.E., Dorsey, D., Klein, R.S., 2010. CXCR4 promotes differentiation of oligodendrocyte progenitors and remyelination. Proc. Natl. Acad. Sci. U.S.A. 107, 11062–11067.
Patel, J.R., Williams, J.L., Muccigrosso, M.M., Liu, L., Sun, T., Rubin, J.B., et al., 2012. Astrocyte TNFR2 is required for CXCL12-mediated regulation of oligodendrocyte progenitor proliferation and differentiation within the adult CNS. Acta Neuropathol. 124, 847–860.
Patel, R., Moore, S., Crawford, D.K., Hannsun, G., Sasidhar, M.V., Tan, K., et al., 2013. Attenuation of corpus callosum axon myelination and remyelination in the absence of circulating sex hormones. Brain Pathol. 23, 462–475.
Pattison, I.H., Jebbett, J.N., 1971. Clinical and histological observations on cuprizone toxicity and scrapie in mice. Res. Vet. Sci. 12, 378–380.
Petratos, S., Gonzales, M.F., Azari, M.F., Marriott, M., Minichiello, R.A., Shipham, K.A., et al., 2004. Expression of the low-affinity neurotrophin receptor, p75(NTR), is upregulated by oligodendroglial progenitors adjacent to the subventricular zone in response to demyelination. Glia 48, 64–75.
Petronilli, V., Zoratti, M., 1990. A characterization of cuprizone-induced giant mouse liver mitochondria. J. Bioenerg. Biomembr. 22, 663–677.
Plant, S.R., Arnett, H.A., Ting, J.P., 2005. Astroglial-derived lymphotoxin-alpha exacerbates inflammation and demyelination, but not remyelination. Glia 49, 1–14.
Plant, S.R., Iocca, H.A., Wang, Y., Thrash, J.C., O'Connor, B.P., Arnett, H.A., et al., 2007. Lymphotoxin beta receptor (Lt betaR): dual roles in demyelination and remyelination and successful therapeutic intervention using Lt betaR-Ig protein. J. Neurosci. 27, 7429–7437.
Plant, S.R., Wang, Y., Vasseur, S., Thrash, J.C., McMahon, E.J., Bergstralh, D.T., et al., 2006. Upregulation of the stress-associated gene p8 in mouse models of demyelination and in multiple sclerosis tissues. Glia 53, 529–537.
Pott, F., Gingele, S., Clarner, T., Dang, J., Baumgartner, W., Beyer, C., et al., 2009. Cuprizone effect on myelination, astrogliosis and microglia attraction in the mouse basal ganglia. Brain Res. 1305, 137–149.
Raasch, J., Zeller, N., van Loo, G., Merkler, D., Mildner, A., Erny, D., et al., 2011. IkappaB kinase 2 determines oligodendrocyte loss by non-cell-autonomous activation of NF-kappaB in the central nervous system. Brain 134, 1184–1198.
Raposo, C., Nunes, A.K., Luna, R.L., Araujo, S.M., da Cruz-Hofling, M.A., Peixoto, C.A., 2013. Sildenafil (Viagra) protective effects on neuroinflammation: the role of iNOS/NO system in an inflammatory demyelination model. Mediators Inflammation 2013, 321460.
Remington, L.T., Babcock, A.A., Zehntner, S.P., Owens, T., 2007. Microglial recruitment, activation, and proliferation in response to primary demyelination. Am. J. Pathol. 170, 1713–1724.
Rossi, L., Lombardo, M.F., Ciriolo, M.R., Rotilio, G., 2004. Mitochondrial dysfunction in neurodegenerative diseases associated with copper imbalance. Neurochem. Res. 29, 493–504.
Russanov, E.M., Ljutakova, S.G., 1980. Effect of cuprizone on copper exchange and superoxide dismutase activity in rat liver. Gen. Pharmacol. 11, 535–538.
Sabo, J.K., Aumann, T.D., Kilpatrick, T.J., Cate, H.S., 2013. Investigation of sequential growth factor delivery during cuprizone challenge in mice aimed to enhance oligodendrogliogenesis and myelin repair. PLoS One 8, e63415.
Sabo, J.K., Aumann, T.D., Merlo, D., Kilpatrick, T.J., Cate, H.S., 2011. Remyelination is altered by bone morphogenic protein signaling in demyelinated lesions. J. Neurosci. 31, 4504–4510.
Sansom, B.F., Pattison, I.H., Jebbett, J.N., 1973. Permeability of blood vessels in mice affected with scrapie or fed with cuprizone. J. Comp. Pathol. 83, 461–466.
Schmidt, H., Raasch, J., Merkler, D., Klinker, F., Krauss, S., Bruck, W., et al., 2009. Type I interferon receptor signalling is induced during demyelination while its function for myelin damage and repair is redundant. Exp. Neurol. 216, 306–311.
Schneider, A., Araujo, G.W., Trajkovic, K., Herrmann, M.M., Merkler, D., Mandelkow, E.M., et al., 2004. Hyperphosphorylation and aggregation of tau in experimental autoimmune encephalomyelitis. J. Biol. Chem. 279, 55833–55839.
Schregel, K., Wuerfel, E., Garteiser, P., Gemeinhardt, I., Prozorovski, T., Aktas, O., et al., 2012. Demyelination reduces brain parenchymal stiffness quantified in vivo by magnetic resonance elastography. Proc. Natl. Acad. Sci. U.S.A. 109, 6650–6655.
Seiwa, C., Yamamoto, M., Tanaka, K., Fukutake, M., Ueki, T., Takeda, S., et al., 2007. Restoration of FcRgamma/Fyn signaling repairs central nervous system demyelination. J. Neurosci. Res. 85, 954–966.
Selvaraju, R., Bernasconi, L., Losberger, C., Graber, P., Kadi, L., Avellana-Adalid, V., et al., 2004. Osteopontin is upregulated during in vivo demyelination and remyelination and enhances myelin formation in vitro. Mol. Cell. Neurosci. 25, 707–721.
Shen, S., Sandoval, J., Swiss, V.A., Li, J., Dupree, J., Franklin, R.J., et al., 2008. Age-dependent epigenetic control of differentiation inhibitors is critical for remyelination efficiency. Nat. Neurosci. 11, 1024–1034.
Silvestroff, L., Bartucci, S., Pasquini, J., Franco, P., 2012. Cuprizone-induced demyelination in the rat cerebral cortex and thyroid hormone effects on cortical remyelination. Exp. Neurol. 235, 357–367.
Silvestroff, L., Bartucci, S., Soto, E., Gallo, V., Pasquini, J., Franco, P., 2010. Cuprizone-induced demyelination in CNP::GFP transgenic mice. J. Comp. Neurol. 518, 2261–2283.
Skripuletz, T., Gudi, V., Hackstette, D., Stangel, M., 2011a. De- and remyelination in the CNS white and grey matter induced by cuprizone: the old, the new, and the unexpected. Histol. Histopathol. 26, 1585–1597.
Skripuletz, T., Hackstette, D., Bauer, K., Gudi, V., Pul, R., Voss, E., et al., 2013. Astrocytes regulate myelin clearance through recruitment of microglia during cuprizone-induced demyelination. Brain 136, 147–167 (A Journal of Neurology).
Skripuletz, T., Miller, E., Grote, L., Gudi, V., Pul, R., Voss, E., et al., 2011b. Lipopolysaccharide delays demyelination and promotes oligodendrocyte precursor proliferation in the central nervous system. Brain Behav. Immun. 25, 1592–1606.
Skripuletz, T., Miller, E., Moharregh-Khiabani, D., Blank, A., Pul, R., Gudi, V., Trebst, C., Stangel, M., 2010. Beneficial effects of minocycline on cuprizone induced cortical demyelination. Neurochem. Res. 35, 1422–1433.
Skuljec, J., Gudi, V., Ulrich, R., Frichert, K., Yildiz, O., Pul, R., et al., 2011. Matrix metalloproteinases and their tissue inhibitors in cuprizone-induced demyelination and remyelination of brain white and gray matter. J. Neuropathol. Exp. Neurol. 70, 758–769.
Song, S.K., Yoshino, J., Le, T.Q., Lin, S.J., Sun, S.W., Cross, A.H., et al., 2005. Demyelination increases radial diffusivity in corpus callosum of mouse brain. NeuroImage 26, 132–140.
Song, S.Y., Kato, C., Adachi, E., Moriya-Sato, A., Inagawa-Ogashiwa, M., Umeda, R., et al., 2007. Expression of an acyl-CoA synthetase, lipidosin, in astrocytes of the

murine brain and its up-regulation during remyelination following cuprizone-induced demyelination. J. Neurosci. Res. 85, 3586–3597.
Soundarapandian, M.M., Selvaraj, V., Lo, U.G., Golub, M.S., Feldman, D.H., Pleasure, D.E., et al., 2011. Zfp488 promotes oligodendrocyte differentiation of neural progenitor cells in adult mice after demyelination. Sci. Rep. 1, 2.
Spencer, J.P., Jenner, P., Daniel, S.E., Lees, A.J., Marsden, D.C., Halliwell, B., 1998. Conjugates of catecholamines with cysteine and GSH in Parkinson's disease: possible mechanisms of formation involving reactive oxygen species. J. Neurochem. 71, 2112–2122.
Stankiewicz, J.M., Brass, S.D., 2009. Role of iron in neurotoxicity: a cause for concern in the elderly? Curr. Opin. Clin. Nutr. Metab. Care 12, 22–29.
Stidworthy, M.F., Genoud, S., Li, W.W., Leone, D.P., Mantei, N., Suter, U., et al., 2004. Notch1 and Jagged1 are expressed after CNS demyelination, but are not a major rate-determining factor during remyelination. Brain 127, 1928–1941.
Stidworthy, M.F., Genoud, S., Suter, U., Mantei, N., Franklin, R.J., 2003. Quantifying the early stages of remyelination following cuprizone-induced demyelination. Brain Pathol. 13, 329–339.
Sun, S.W., Liang, H.F., Trinkaus, K., Cross, A.H., Armstrong, R.C., Song, S.K., 2006. Non-invasive detection of cuprizone induced axonal damage and demyelination in the mouse corpus callosum. Magn. Reson. Med. 55, 302–308.
Suzuki, K., 1969. Giant hepatic mitochondria: production in mice fed with cuprizone. Science 163, 81–82.
Tanaka, T., Murakami, K., Bando, Y., Yoshida, S., 2013. Minocycline reduces remyelination by suppressing ciliary neurotrophic factor expression after cuprizone-induced demyelination. J. Neurochem. 127, 259–270.
Tandler, B., Hoppel, C.L., 1973. Division of giant mitochondria during recovery from cuprizone intoxication. J. Cell Biol. 56, 266–272.
Tandler, B., Hoppel, C.L., 1975. The failure of supplemental dietary copper to prevent cuprizone-induced alterations in mouse hepatocytes. Beitr Pathol. 156, 56–64.
Tansey, F.A., Zhang, H., Cammer, W., 1996. Expression of carbonic anhydrase II mRNA and protein in oligodendrocytes during toxic demyelination in the young adult mouse. Neurochem. Res. 21, 411–416.
Tansey, F.A., Zhang, H., Cammer, W., 1997. Rapid upregulation of the Pi isoform of glutathione-*S*-transferase in mouse brains after withdrawal of the neurotoxicant, cuprizone. Mol. Chem. Neuropathol. 31, 161–170.
Taylor, L.C., Gilmore, W., Ting, J.P., Matsushima, G.K., 2010a. Cuprizone induces similar demyelination in male and female C57BL/6 mice and results in disruption of the estrous cycle. J. Neurosci. Res. 88, 391–402.
Taylor, L.C., Puranam, K., Gilmore, W., Ting, J.P., Matsushima, G.K., 2010b. 17beta-Estradiol protects male mice from cuprizone-induced demyelination and oligodendrocyte loss. Neurobiol. Dis. 39, 127–137.
Tezuka, T., Tamura, M., Kondo, M.A., Sakaue, M., Okada, K., Takemoto, K., et al., 2013. Cuprizone short-term exposure: astrocytic IL-6 activation and behavioral changes relevant to psychosis. Neurobiol. Dis. 59, 63–68.
Tobin, J.E., Xie, M., Le, T.Q., Song, S.K., Armstrong, R.C., 2011. Reduced axonopathy and enhanced remyelination after chronic demyelination in fibroblast growth factor 2 (Fgf2)-null mice: differential detection with diffusion tensor imaging. J. Neuropathol. Exp. Neurol. 70, 157–165.
Trapp, B.D., Nishiyama, A., Cheng, D., Macklin, W., 1997. Differentiation and death of premyelinating oligodendrocytes in developing rodent brain. J. Cell Biol. 137, 459–468.
Trebst, C., Heine, S., Lienenklaus, S., Lindner, M., Baumgartner, W., Weiss, S., et al., 2007. Lack of interferon-beta leads to accelerated remyelination in a toxic model of central nervous system demyelination. Acta Neuropathol. 114, 587–596.
Troadec, J.D., Marien, M., Darios, F., Hartmann, A., Ruberg, M., Colpaert, F., et al., 2001. Noradrenaline provides long-term protection to dopaminergic neurons by reducing oxidative stress. J. Neurochem. 79, 200–210.
Tsiperson, V., Li, X., Schwartz, G.J., Raine, C.S., Shafit-Zagardo, B., 2010. GAS6 enhances repair following cuprizone-induced demyelination. PLoS One 5, e15748.
Van Strien, M.E., Baron, W., Bakker, E.N., Bauer, J., Bol, J.G., Breve, J.J., et al., 2011. Tissue transglutaminase activity is involved in the differentiation of oligodendrocyte precursor cells into myelin-forming oligodendrocytes during CNS remyelination. Glia 59, 1622–1634.
Vana, A.C., Flint, N.C., Harwood, N.E., Le, T.Q., Fruttiger, M., Armstrong, R.C., 2007. Platelet-derived growth factor promotes repair of chronically demyelinated white matter. J. Neuropathol. Exp. Neurol. 66, 975–988.
Venturini, G., 1973. Enzymic activities and sodium, potassium and copper concentrations in mouse brain and liver after cuprizone treatment in vivo. J. Neurochem. 21, 1147–1151.
Veto, S., Acs, P., Bauer, J., Lassmann, H., Berente, Z., Setalo Jr., G., et al., 2010. Inhibiting poly(ADP-ribose) polymerase: a potential therapy against oligodendrocyte death. Brain 133, 822–834.
VonDran, M.W., Singh, H., Honeywell, J.Z., Dreyfus, C.F., 2011. Levels of BDNF impact oligodendrocyte lineage cells following a cuprizone lesion. J. Neurosci. 31, 14182–14190.
Voss, E.V., Skuljec, J., Gudi, V., Skripuletz, T., Pul, R., Trebst, C., et al., 2012. Characterisation of microglia during de- and remyelination: can they create a repair promoting environment? Neurobiol. Dis. 45, 519–528.
Wagner, T., Rafael, J., 1977. Biochemical properties of liver megamitochondria induced by chloramphenicol or cuprizone. Exp. Cell Res. 107, 1–13.
Wakabayashi, T., 2002. Megamitochondria formation—physiology and pathology. J. Cell. Mol. Med. 6, 497–538.
Wakabayashi, T., Asano, M., Ishikawa, K., Kishimoto, H., 1977. Cuprizone-induced megamitochondrial formation and membrane fusion. J. Electron Microsc. (Tokyo) 26, 137–140.
Wakabayashi, T., Asano, M., Ishikawa, K., Kishimoto, H., 1978. Mechanism of the formation of megamitochondria by copper-chelating agents. V. Further studies on isolated megamitochondria. Acta Pathol. Jpn. 28, 215–223.
Wakabayashi, T., Asano, M., Kurono, C., 1975. Mechanism of the formation of megamitochondria induced by copper-chelating agents, II. Isolation and some properties of megamitochondria from the cuprizone-treated mouse liver. Acta Pathol. Jpn. 25, 39–49.
Wang, H., Li, C., Mei, F., Liu, Z., Shen, H.Y., Xiao, L., 2013. Cuprizone-induced demyelination in mice: age-related vulnerability and exploratory behavior deficit. Neurosci. Bull. 29, 251–259.
Witherick, J., Wilkins, A., Scolding, N., Kemp, K., 2010. Mechanisms of oxidative damage in multiple sclerosis and a cell therapy approach to treatment. Autoimmune Dis. 2011, 164608.
Woodruff, R.H., Fruttiger, M., Richardson, W.D., Franklin, R.J., 2004. Platelet-derived growth factor regulates oligodendrocyte progenitor numbers in adult CNS and their response following CNS demyelination. Mol. Cell. Neurosci. 25, 252–262.
Wu, Q.Z., Yang, Q., Cate, H.S., Kemper, D., Binder, M., Wang, H.X., et al., 2008. MRI identification of the rostral–caudal pattern of pathology within the corpus callosum in the cuprizone mouse model. J. Magn. Reson. Imaging: JMRI 27, 446–453.
Xu, C., Bailly-Maitre, B., Reed, J.C., 2005. Endoplasmic reticulum stress: cell life and death decisions. J. Clin. Invest. 115, 2656–2664.
Xu, H., Yang, H.J., Li, X.M., 2013. Differential effects of antipsychotics on the development of rat oligodendrocyte precursor cells exposed to cuprizone. Eur. Arch. Psychiatry Clin. Neurosci. 264, 121–129.
Xu, H., Yang, H.J., McConomy, B., Browning, R., Li, X.M., 2010. Behavioral and neurobiological changes in C57BL/6 mouse exposed to cuprizone: effects of antipsychotics. Front. Behav. Neurosci. 4, 8.
Xu, H., Yang, H.J., Rose, G.M., Li, X.M., 2011. Recovery of behavioral changes and compromised white matter in C57BL/6 mice exposed to cuprizone: effects of antipsychotic drugs. Front. Behav. Neurosci. 5, 31.
Xu, H., Yang, H.J., Zhang, Y., Clough, R., Browning, R., Li, X.M., 2009. Behavioral and neurobiological changes in C57BL/6 mice exposed to cuprizone. Behav. Neurosci. 123, 418–429.
Ye, J.N., Chen, X.S., Su, L., Liu, Y.L., Cai, Q.Y., Zhan, X.L., et al., 2013. Progesterone alleviates neural behavioral deficits and demyelination with reduced degeneration of oligodendroglial cells in cuprizone-induced mice. PloS One 8, e54590.
Yoshikawa, K., Palumbo, S., Toscano, C.D., Bosetti, F., 2011. Inhibition of 5-lipoxygenase activity in mice during cuprizone-induced demyelination attenuates neuroinflammation, motor dysfunction and axonal damage. Prostaglandins Leukot. Essent. Fatty Acids 85, 43–52.
Yu, O., Steibel, J., Mauss, Y., Guignard, B., Eclancher, B., Chambron, J., et al., 2004. Remyelination assessment by MRI texture analysis in a cuprizone mouse model. Magn. Reson. Imaging 22, 1139–1144.
Zaaraoui, W., Deloire, M., Merle, M., Girard, C., Raffard, G., Biran, M., et al., 2008. Monitoring demyelination and remyelination by magnetization transfer imaging in the mouse brain at 9.4 T. MAGMA 21, 357–362.
Zatta, P., Raso, M., Zambenedetti, P., Wittkowski, W., Messori, L., Piccioli, F., et al., 2005. Copper and zinc dismetabolism in the mouse brain upon chronic cuprizone treatment. Cell. Mol. Life Sci. 62, 1502–1513.
Zendedel, A., Beyer, C., Kipp, M., 2013. Cuprizone-induced demyelination as a tool to study remyelination and axonal protection. J. Mol. Neurosci.: MN 51, 567–572.
Zhang, J., Jones, M.V., McMahon, M.T., Mori, S., Calabresi, P.A., 2011. In vivo and ex vivo diffusion tensor imaging of cuprizone-induced demyelination in the mouse corpus callosum. Magn Reson Med. 67, 750–759.
Zhang, L., Yu, W., Schroedter, I., Kong, J., Vrontakis, M., 2012. Galanin transgenic mice with elevated circulating galanin levels alleviate demyelination in a cuprizone-induced MS mouse model. PLoS One 7, e33901.
Zhang, Y., Xu, H., Jiang, W., Xiao, L., Yan, B., He, J., et al., 2008. Quetiapine alleviates the cuprizone-induced white matter pathology in the brain of C57BL/6 mouse. Schizophr. Res. 106, 182–191.
Zhou, Y.X., Pannu, R., Le, T.Q., Armstrong, R.C., 2012. Fibroblast growth factor 1 (FGFR1) modulation regulates repair capacity of oligodendrocyte progenitor cells following chronic demyelination. Neurobiol. Dis. 45, 196–205.
Zoupi, L., Markoullis, K., Kleopa, K.A., Karagogeos, D., 2013. Alterations of juxtaparanodal domains in two rodent models of CNS demyelination. Glia 61, 1236–1249.